AR-010-203

DSTO-TR-0523

Stress Analysis of a Plate Containing a Round Hole with Combined Cold Expansion and Interference Fitting Under F-111C Representative Loading Conditions

R.B. Allan and M. Heller

] APPROVED FOR PUBLIC RELEASE

DEPARTMENT ◆ OF DEFENCE

DEFENCE SCIENCE AND TECHNOLOGY ORGANISATION

Stress Analysis of a Plate Containing a Round Hole with Combined Cold Expansion and Interference Fitting Under F-111C Representative Loading Conditions

R.B. Allan and M. Heller

Airframes and Engines Division
Aeronautical and Maritime Research Laboratory

DSTO-TR-0523

ABSTRACT

This investigation has been undertaken as part of a program of work having the aim of determining a suitable fatigue life enhancement option for the non-circular fuel flow vent hole # 13 in the wing pivot fitting of the F-111C aircraft. The stress analysis has been undertaken using two dimensional finite element methods assuming either elastic-perfectly plastic or strain hardening material behaviour models. The effect on critical plate stresses due to enhancement by cold expansion and interference fitting, used separately or together, has been quantified in the presence of representative cold proof test loading and a sample remote spectrum loading. For all enhancement cases considered, irrespective of material model, the stress response during the sample remote loading was linear, with a cyclic stress concentration factor of unity. Enhancement through combined cold expansion and interference fitting was considered a great deal better than interference fitting only. For example, the combined enhancement of 1.5% cold expansion followed by 0.5% interference fitting, as compared to 0.5% interference fitting only, led to a change in critical hoop stress from 350 MPa to -1080 MPa. These favourable results indicate that such an enhancement procedure would potentially be suitable for extending the fatigue life of the F-111 #13 fuel flow vent hole region, pending the results of an investigation on a non-circular hole geometry currently in progress.

RELEASE LIMITATION

Approved for public release

DEPARTMENT OF DEFENCE

DEFENCE SCIENCE AND TECHNOLOGY ORGANISATION

Published by

DSTO Aeronautical and Maritime Research Laboratory
PO Box 4331
Melbourne Victoria 3001

Telephone: (03) 9626 7000
Fax: (03) 9626 7999

AR-010-203
April 1997

APPROVED FOR PUBLIC RELEASE

Stress Analysis of a Plate Containing a Round Hole with Combined Cold Expansion and Interference Fitting Under F-111C Representative Loading Conditions

Executive Summary

An area of major concern for the F-111 airframe in service with the RAAF is the wing pivot fitting in which there are a number of non-circular (elongated) machined fuel flow vent holes. There have been numerous incidents of fatigue cracks at fuel flow vent hole #13 in the wing pivot fitting, and the problem could compromise the structural integrity of the F-111 fleet out to the planned withdrawal date of approximately 2020. Currently, this problem is being managed by reshaping periodically, the fuel flow vent holes to one of a family of progressively larger shapes, thereby removing any existing cracks. Unfortunately, this process does not completely eliminate further cracking, and at the current rate of crack growth and hole reshaping, this method may not be sufficient to enable these aircraft to reach their desired service life.

This present investigation has been undertaken as part of a program of work having the aim of determining a suitable fatigue life enhancement option for the non-circular fuel flow vent hole # 13 in the wing pivot fitting of the F-111C aircraft. The stress analysis has been undertaken using two dimensional finite element methods assuming either elastic-perfectly plastic or strain hardening material behaviour models. The effect on critical plate stresses due to enhancement by cold expansion and interference fitting, used separately or together, has been quantified in the presence of representative cold proof test loading and a sample remote spectrum loading. For all enhancement cases considered, irrespective of material model, the stress response during the sample remote loading was linear, with a cyclic stress concentration factor of unity. Enhancement through combined cold expansion and interference fitting was considered a great deal better than interference fitting only. For example, the combined enhancement of 1.5% cold expansion followed by 0.5% interference fitting, as compared to 0.5% interference fitting only, led to a change in critical hoop stress from 350 MPa to -1080 MPa.

These favourable results indicate that such an enhancement procedure would potentially be suitable for extending the fatigue life of the F-111 #13 fuel flow vent hole region, pending the results of an investigation on a non-circular hole geometry currently in progress.

Authors

R.B. Allan

Airframes and Engines Division

Robert Allan completed a B.E. (Aeronautical) at R.M.I.T. in 1978. Since then he has worked in the areas of aircraft structural design, repair and manufacturing at major Australian and U.S. aircraft companies. Some major projects worked on in this time were the tailplane and elevator design of the Wamira aircraft project, F-18 aft fuselage redesign and the support of local manufacture of numerous aircraft components. Prior to joining AMRL in 1994, he spent 5 years in the field of polymer flow characterisation and simulation using finite element methods gaining a broad knowledge of finite element stress analysis. Since joining AMRL he has worked in the area of life extension through the use of structural mechanics in support of Australian Defence Force aircraft, specialising in finite element stress analysis and advanced experimental stress analysis.

M. Heller

Airframes and Engines Division

Manfred Heller completed a B. Eng. (Hons.) in Aeronautical Engineering at the University of New South Wales in 1981. He was awarded a Department of Defence Postgraduate Cadetship in 1986, completing a PhD at Melbourne University in 1989. He commenced work in Structures Division at the Aeronautical Research Laboratory in 1982. He has an extensive publication record focussing on the areas of stress analysis, fracture mechanics, fatigue life extension methodologies and experimental validation. Since 1992 he has led tasks which develop and evaluate techniques for extending the fatigue life of ADF aircraft components and provide specialised structural mechanics support to the ADF. He is currently a Senior Research Scientist in the Airframes and Engines Division.

Contents

Notation

σ	stress
ρ	re-yield radius
ν	Poisson's Ratio
λ	dimensionless interference, δ/a
δ	radial interference ($\delta=r_m-a$)
a	hole radius
b	annulus outside radius
c	elastic-plastic boundary
E	elastic modulus
GPa	giga pascals
g	ratio of annulus modulus to mandrel modulus
mm	millimetres
MPa	mega pascals
r	radius
u	radial displacement of node on mandrel/hole boundary
v	hoop displacement of node on mandrel/hole boundary
x, y	cartesian co-ordinates

Subscripts

θ	hoop
m	mandrel
p	plate
r	radial
0	yield

Superscripts

CE	Cold expansion

List of Abbreviations

AMRL	Aeronautical and Maritime Research Laboratory
CPLT	cold proof load test
CE	cold expansion
DADTA	durability and damage tolerance analysis
EPPM	elastic-perfectly plastic material
FE	finite element
FFVH	fuel flow vent hole
FFVH13	fuel flow vent hole number 13
IF	interference fitting
RAAF	Royal Australian Air Force
SHM	strain hardening material

1. Introduction

An area of major concern in the F-111C airframe is the wing pivot fitting manufactured from D6ac steel, in which there are a number of machined fuel flow vent holes (FFVH), see Figure 1. Under cold proof load tests, the material around one of these holes, FFVH13, experiences extensive plastic deformation, which results in the introduction of tensile residual stresses. These residual stresses coupled with the local material response due to the remote loading sequence are detrimental, and contribute to crack initiation and growth at the affected area. There have been numerous incidents of fatigue cracking at FFVH13 in the wing pivot fitting in the RAAF's F-111C fleet, and the problem could compromise the structural integrity of these aircraft out to the planned withdrawal date of 2020.

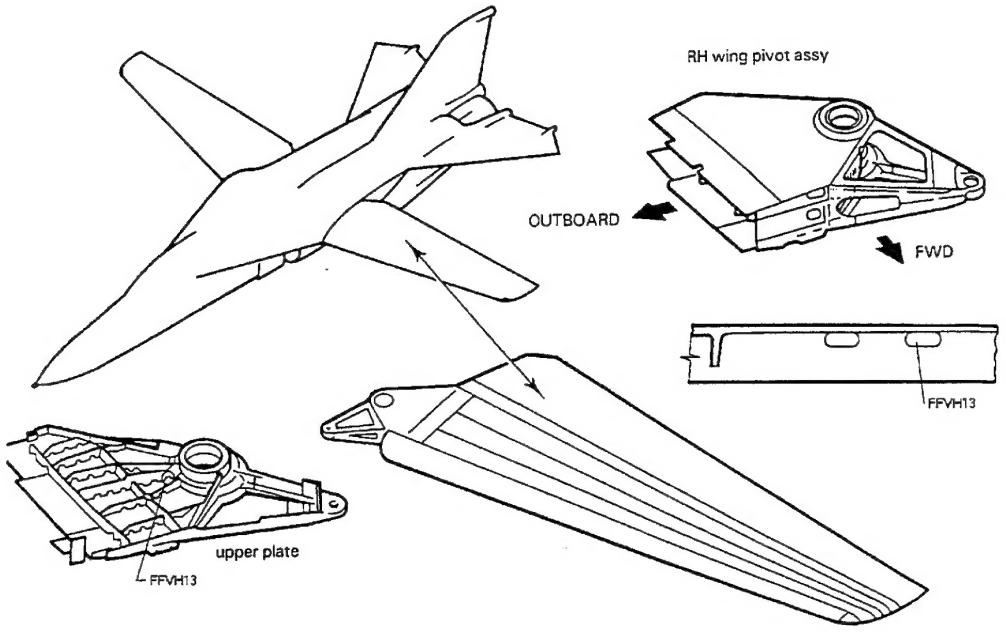

Figure 1: F-111 Aircraft & wing, showing location of critical hole (FFVH13)

Currently, the problem is being managed by reworking the elongated fuel flow vent holes to a family of progressively larger shapes [1]. This process removes small cracks and corrosion as detected. The extent of the rework depends on the size of the detected crack. Unfortunately, the reworking does not completely eliminate further cracking, and at the current rate of crack growth and reworking, this method may not be sufficient to enable the aircraft to reach its desired service life. A durability and damage tolerance analysis (DADTA) is presently being used to certify the use of these rework shapes as a valid means for managing this critical location. If the reworking

procedure cannot allow the aircraft to reach the desired service life, an alternative method of life extension will be required. In view of this problem, AMRL has been tasked with the development of a proposed non-circular cold expansion/interference fit plug option, for the life extension of FFVH13, with the aim of eliminating crack growth or significantly reducing the crack growth rate.

The typical benefit of cold expansion and/or interference fitting for the life extension of plates containing circular holes is reasonably well established and documented. For example, the use of interference fitting and/or cold expansion has been reviewed by Mann and Jost [2]. Closed form theoretical solutions only apply to the simplest configurations, so typically finite element analyses are employed to solve problems of practical importance. However previous work does not give clear guidelines for either: (i) non-circular geometries, or (ii) complex remote loading conditions and realistic strain hardening material properties. Both of these issues need to be addressed when developing a life extension option for the FFVH13 on the F-111 aircraft.

In this report we address the second issue for a circular hole case, as a precursor to the analysis of the more complex non-circular case. The key parameters in this investigation have been chosen to be representative of the Wing Pivot Fitting region of the F-111C aircraft. In Section 2 the process definitions for cold expansion and interference fitting are given, and their effect on stresses at the hole edge is explained generically. The finite element methodology employed in this report is then presented in Section 3. The results of benchmark analyses are then given in Section 4, where a comparison between closed-form theoretical and elastic-perfectly plastic finite element analyses is made, for annuli having material properties representative of aluminium alloy or steel. In Section 5 the problem of a rectangular plate containing a circular hole that is cold expanded and interference fitted is examined. Here both elastic-perfectly plastic and strain hardening material property cases are considered, and the plate stress response under remote CPLT and sample remote spectrum loading is presented.

2. Cold Expansion and Interference Fitting Process Definitions

For the case of a plate containing an enhanced circular hole it is helpful to highlight the major differences between cold expansion and interference-fitting, (see also Broek [3] and Jost [4,5]) as follows.

In the ***Cold expansion*** (CE) process, the hole is initially expanded to a level sufficient to cause local yielding to occur. This is typically achieved by passage of an oversize tapered mandrel or mandrel/sleeve combination through the hole. Then the mandrel is removed from the hole, and the surrounding elastically deformed material forces a reduction in hole diameter from the fully expanded size. This results in a zone around the hole containing residual compressive hoop stresses. As the extent of yielding

during expansion is increased, the larger is the zone of induced compressive stress. Depending on the degree of expansion, compressive reyielding on mandrel removal can also occur, although the size of this reyielded zone is substantially less than that generated by the mandrel enlarging the hole. Under the influence of cyclic remote loading, the presence of the compressive zone at the hole boundary results in the mean value of the induced local cyclic stresses to be significantly less than for a non-cold expanded hole. Although the magnitude of the local cyclic stress range is typically unchanged as compared to the non cold expanded hole, the tensile part of the cycle is substantially reduced. Hence the reduction in mean local stress at the hole boundary is typically highly beneficial in delaying the onset of crack initiation and therefore increasing the fatigue life of a component with a cold expanded hole.

Interference fitting (IF) is the process of installing an oversized mandrel into the hole, often achieved by passage of a tapered mandrel into the hole until a required interference level is obtained. Unlike the cold expansion process, the mandrel remains *in situ* and typically plate deformation around the hole due to the interference fitting process is elastic. This process has two effects. Firstly, a residual tensile circumferential stress is induced in the plate at the hole boundary. Secondly, the *in situ* mandrel provides an alternative load path when the plate is subjected to remote cyclic loading, thereby reducing the magnitude of local cyclic stresses in the plate at the hole boundary. Typically, the reduction in the magnitude of the local cyclic stresses is highly beneficial in delaying the onset of crack initiation and hence increasing fatigue life. However caution must be exercised when assessing the potential benefit of this approach, particularly if the remote loading sequence is dominated by compressive loads. In such a case, even though the magnitude of local cyclic stress at the hole edge is reduced, the higher mean stress due interference fitting signifies that both applied tensile loading and compressive loading will be fatigue damaging. Hence the potential improvement in fatigue life of a component with an interference fitted hole will depending on the particular remote loading sequence, and on the magnitude of the mean stress due to interference fitting.

Based on the above preceding descriptions, it is expected that greatest benefit to fatigue life extension will result from a combination of cold expansion and interference fitting.

3. Finite Element Method

In this work, elastic and plastic plane strain analyses have been undertaken using the PAFEC finite element code, level 8 running on a Hewlett Packard K series 9000 computer at AMRL. Eight-noded isoparametric quadrilateral elements (PAFEC type 36210) were used for all analyses The plasticity subroutines in PAFEC make use of the Prandtl-Reuss equations in conjunction with the von Mises yield criterion and an isotropic hardening model. For all plastic analyses loads were applied incrementally, with further iterations undertaken for each increment until acceptable convergence to

the material non-linear stress-strain constitutive response curve was achieved. The convergence criteria was judged to be achieved when the internal energy was less than 1% different to the external work due to the applied loads, for a given increment.

3.1 Geometries and Typical Meshes

The notation and geometry relevant to the two dimensional idealisation of the cold expansion of an annulus is given in Figure 2. The outer radius of the annulus is denoted as b and its initial inner radius is denoted as a. An oversize mandrel of radius r_m is inserted in the hole. The resultant hole expansion causes local yielding in the annulus to occur, and the extent of yielding is defined by the elastic plastic boundary c. Upon removal of the mandrel from the hole the surrounding elastically deformed material forces a reduction in hole diameter from the fully expanded size. Depending on the degree of expansion, compressive reyielding on mandrel removal can also occur, and the size of this reyielded zone (which is substantially less than that generated by the mandrel enlarging the hole) is denoted as p.

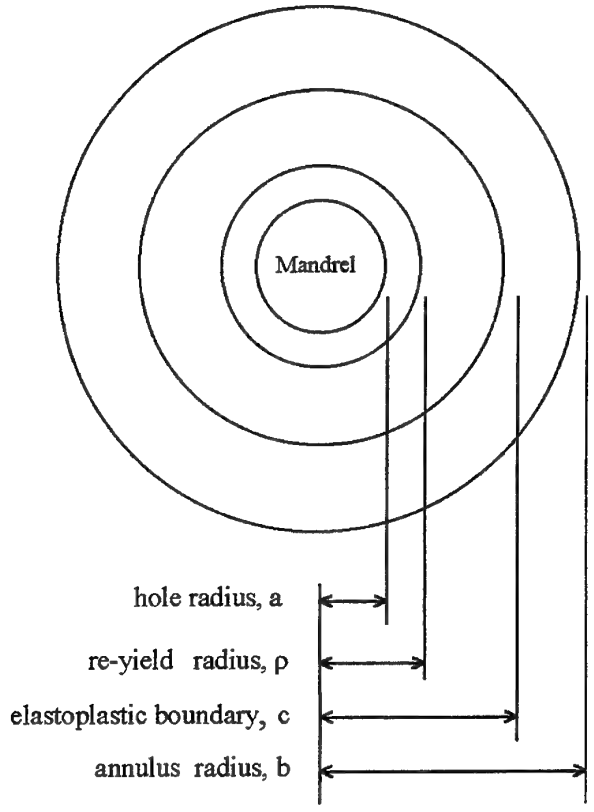

Figure 2: Notation and geometry relevant to annulus undergoing cold expansion.

Figure 3 shows the mesh used for the finite element analysis of the annulus, which is not subjected to remote loading. Due to the axi-symmetric nature of the annulus, and with the application of appropriate boundary conditions, it was only necessary to model a small (2.5°) segment of the original geometry. The following boundary conditions were applied to the mesh: (i) for all nodes on the line defined by θ=0°, the displacement in the direction normal to this line was constrained, and (ii) for all nodes on the line θ=2.5°, displacement in the direction normal to this line were constrained. A typical PAFEC input data file for this model is given in Appendix A.

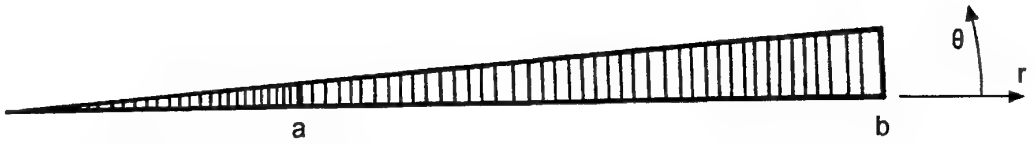

Figure 3: Typical finite element mesh for annulus segment

The geometry relevant to the two dimensional idealisation of the cold expansion of a circular hole in a rectangular plate is shown in Figure 4. Here the plate is of width 2w, length 2h, and has a centrally located circular hole of diameter 2r. The analysis of the rectangular plate geometry allows a realistic remote load (i.e. uniaxial) to be applied to plate with a cold expanded hole. Due to symmetry, only one quarter of the plate was modelled as shown in Figures 5 and 6. The following constraint boundary conditions were applied to the mesh: (i) for all nodes on the x axis, displacement in the y direction was constrained, and (ii) for all nodes on the y axis, displacement in the x direction was constrained. A typical PAFEC input data file for this model is given in Appendix B.

3.2 Modelling of Interference Fit and Cold Expansion

3.2.1 Elastic Interference Cases

The formulation of the required interference constraint conditions in the finite element model can be described by considering two typical adjacent points (A and B) on the mandrel/plate interface, as shown prior to sleeve insertion in Figure 7. After insertion these two points become coincident for the no slip (i.e. no relative displacement in the tangential direction) case. Hence the constraint equations in terms of Cartesian displacements per pair of nodes for this case are given in Equations (1) and (2). These equations are then used for all pairs of nodes around the interface. In the case of slip allowed, only the constraint condition given in equation (1) is used. This enables relative displacement in the hoop direction to occur between corresponding nodes at the mandrel and hole interface.

$$u_p - u_m = \delta \tag{1}$$

$$v_p - v_m = 0 \tag{2}$$

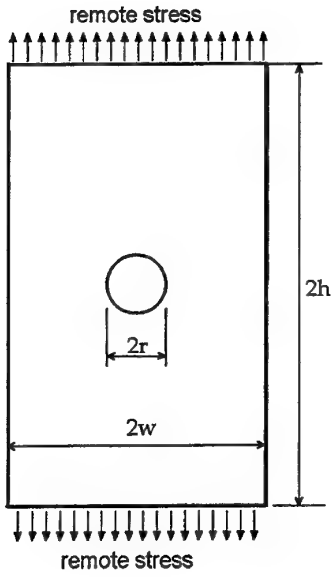

Figure 4: Notation and geometry for rectangular plate containing a circular hole

It should be noted that the magnitude of the local cyclic stresses due to remote loading are independent of the stresses generated by the applied interference (assuming full contact and no tangential slip at the mandrel/plate interface). Hence the total stress at a given point in the plate is determined simply by adding the cyclic stress and the stress due to the interference.

3.2.2 Plastic Cases

The plastic analyses for cold expansion and interference fitting were undertaken in a similar manner to the elastic analyses except that the expansion constraint conditions and remote loading was applied in small increments. The only difficulty that arises in using this method is specifying correctly the increment that corresponds to mandrel removal (ie cold expansion removal) for geometries other than the annulus. For the plate geometries which are non-axi-symmetric the hole would end up non-circular after cold expansion. During the iterative finite element analysis, the increment in the cold expansion cycle considered "mandrel removal" was taken to be when the radial stress at the critical location (θ=0°) becomes zero. The relatively small error arising from this assumption, as a function of angular position, is shown in Figure 8 for the typical case of a cold expanded hole as considered in Section 5.4. Here the maximum error is 32.7 MPa, and occurs at θ=90°. For comparison purposes, the corresponding residual hoop and maximum radial stresses are also shown in this figure.

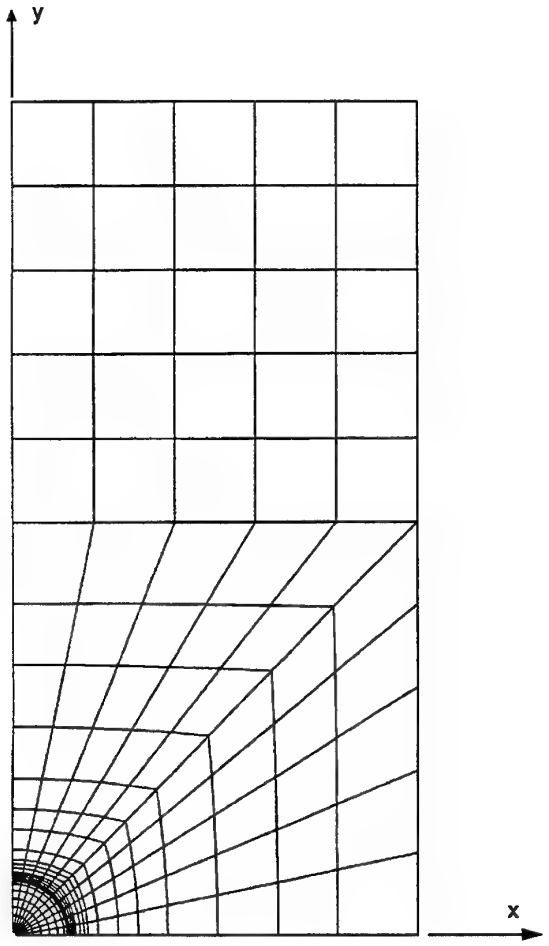

Figure 5: Typical overall finite element mesh for modelling a rectangular plate containing a circular hole

3.2.3 General Comments

The analysis procedure presented above is considered valid for the assumed constraint conditions, with the further requirement that no separation at the mandrel/plate interface occurs during remote loading of the plate. In practice these requirements will depend on interference level, the relative material stiffness values of the mandrel and plate, the coefficient of friction at the mandrel/hole interface, and the magnitude of the remote loading.

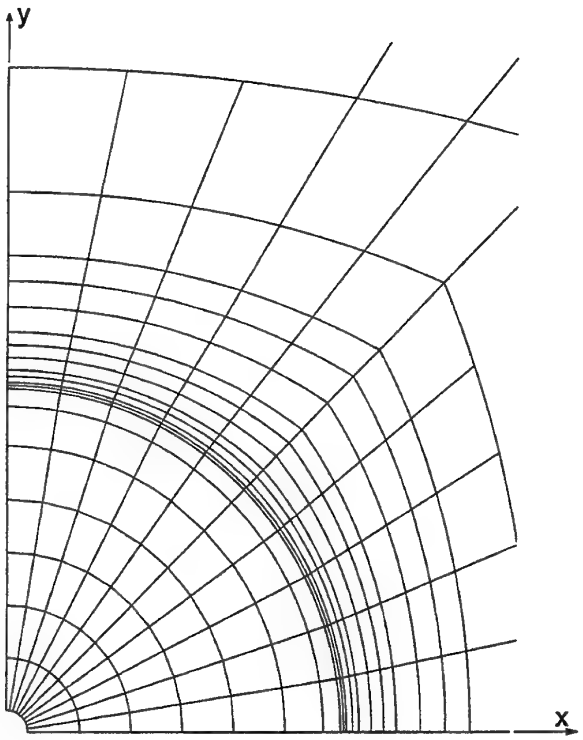

Figure 6: Typical finite element mesh near region of hole boundary for rectangular plate case

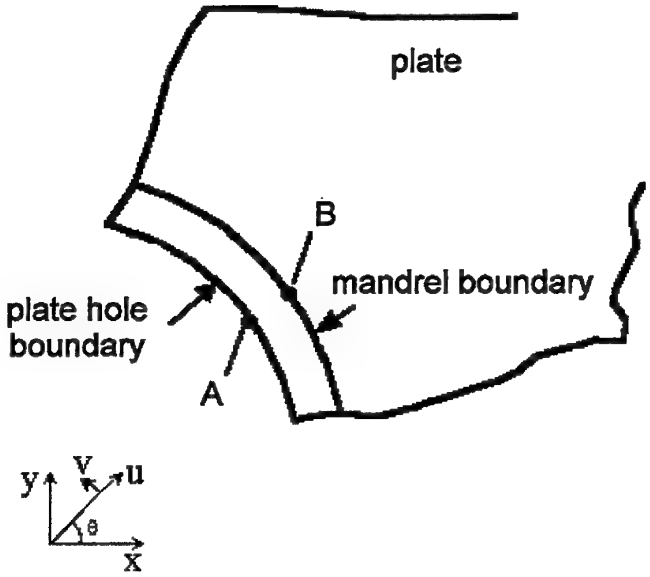

Figure 7: Generic geometry for definition of interference fit boundary conditions along mandrel/plate interface

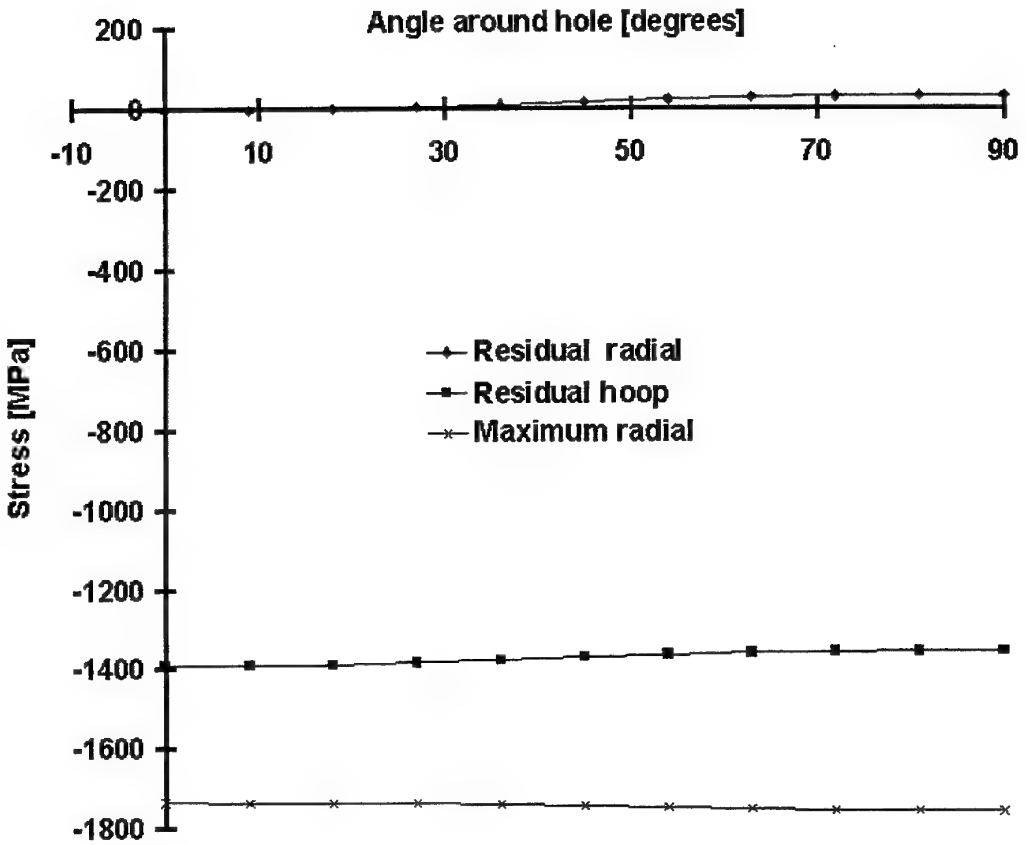

Figure 8: Stress variation around hole boundary: for case presented in Section 5.4: (i) radial stress at the maximum cold expansion level, and (ii) residual radial and hoop stresses at completion of cold expansion.

3.3 Elastic-Plastic Material Properties

Analyses undertaken for D6ac steel (F-111C wing pivot fitting material) used one of the following two non-linear material constitutive response curves: (i) an elastic-perfectly plastic response to enable direct comparison of finite element results with closed-form theoretical solutions, or (ii) a strain hardening response to allow more realistic simulation of true material characteristics. These two curves are shown in Figure 9. Some preliminary analyses were also performed with aluminium plate material, assuming an elastic-perfectly plastic response, with an elastic modulus of 69 GPa and a yield point of 480 MPa.

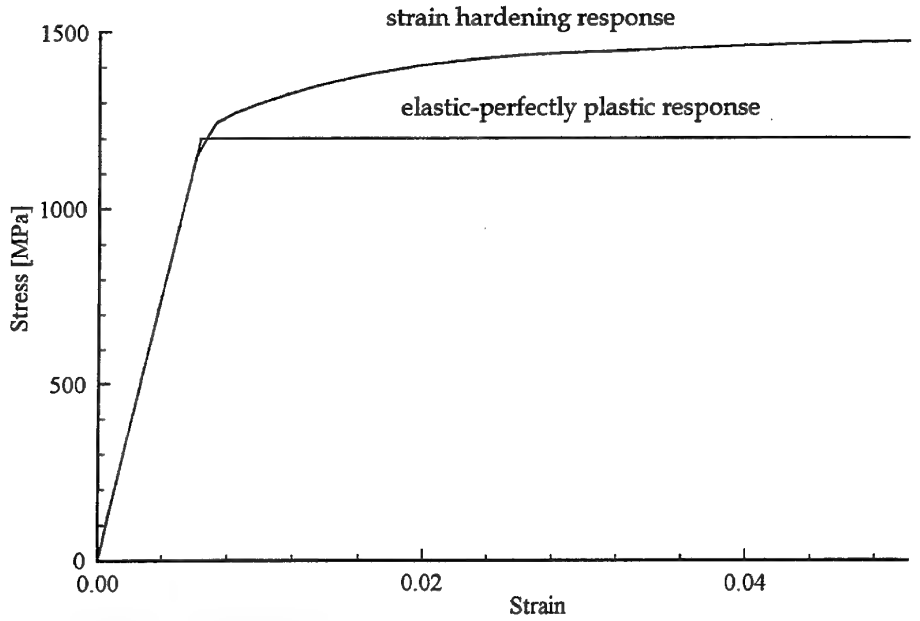

Figure 9: Assumed elastic-perfectly plastic and strain hardening material constitutive responses of D6ac steel.

4. Benchmark Finite Element Analyses

The following three plane-strain analyses were undertaken to allow comparison of typical finite element results with theoretical solutions.

1. Elastic analysis of a large rectangular aluminium plate with an interference fitting of 1% due to a steel mandrel.
2. Elastic-perfectly plastic analysis of an aluminium annulus with an interference fitting of 4% due to a steel mandrel.
3. Elastic-perfectly plastic analysis of a steel annulus with cold expansion to 1.5 %, followed by 0.5% interference fitting due to a steel mandrel.

4.1 Elastic Analysis of a Large Rectangular Aluminium Plate with a 1% Interference Fitted Steel Mandrel

For this analysis the plate geometry as shown in Figure 4 was considered, with a hole diameter of 20 mm, plate length of 400 mm, and plate width of 200 mm. The plate material was an aluminium alloy with properties E_p=72.4 MPa, and ν_p=0.33. The mandrel material was steel with properties E_m=209 GPa and ν_m= 0.33. The plate was loaded with a remote stress of 100 MPa and fitted with a 1% interference steel mandrel.

The results for peak radial and hoop stresses in the plate and the hole edge were within 2% of those obtained in prior work [6].

4.2 Elastic-Perfectly Plastic Analysis of an Aluminium Annulus with a 4% Interference Fitted Steel Mandrel

This case was chosen to allow for comparison of the finite element results and the closed form solutions presented in Reference 4. The plate geometry as shown in Figure 2 was considered, with material properties, E_p = 69 GPa, υ_p=0.33, σ_0 = 480 MPa, and geometric parameters, a = 10 mm, and b = 100 mm,. The mandrel elastic material properties were E_m = 209 GPa and υ_m=0.3. The 2.5° annulus segment finite element model as shown in Figure 3 was used. The mandrel was represented by 120 divisions, and the annulus by 400 divisions. To model the interference-fitting, the constraint conditions were applied incrementally as follows: one increment of 0.3808% interference followed by eight increments of 0.0544% interference and then fourteen increments of 0.136% interference. The large first increment was used to get up to just below the yield condition, and then followed by smaller increments to get past the yield point. Good correlation between the finite element results and the theoretical predictions [4] was obtained, as indicated in Figure 10.

The location of the elastic-plastic boundary at the 4% interference level is illustrated in Figure 11, which shows the von Mises stress distribution in the annulus from the hole edge to the annulus outside diameter.

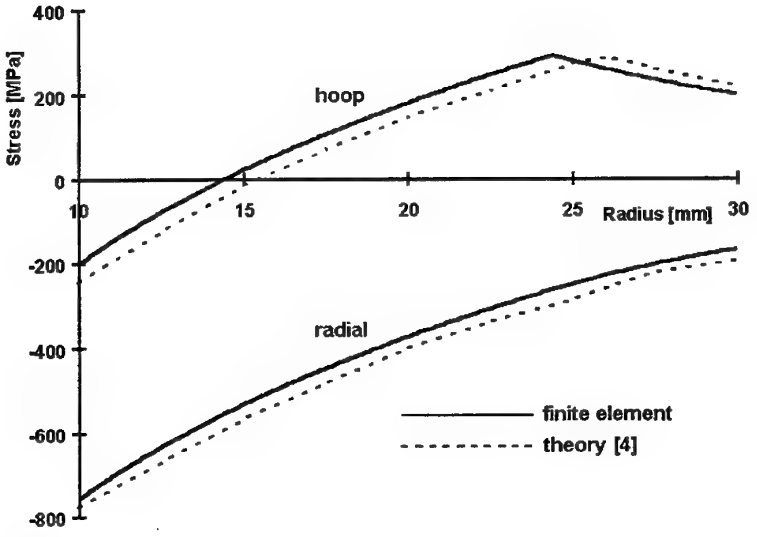

Figure 10: Comparison of results for hoop and radial stresses for an interference fitted steel mandrel in an aluminium annulus at a 4% interference level

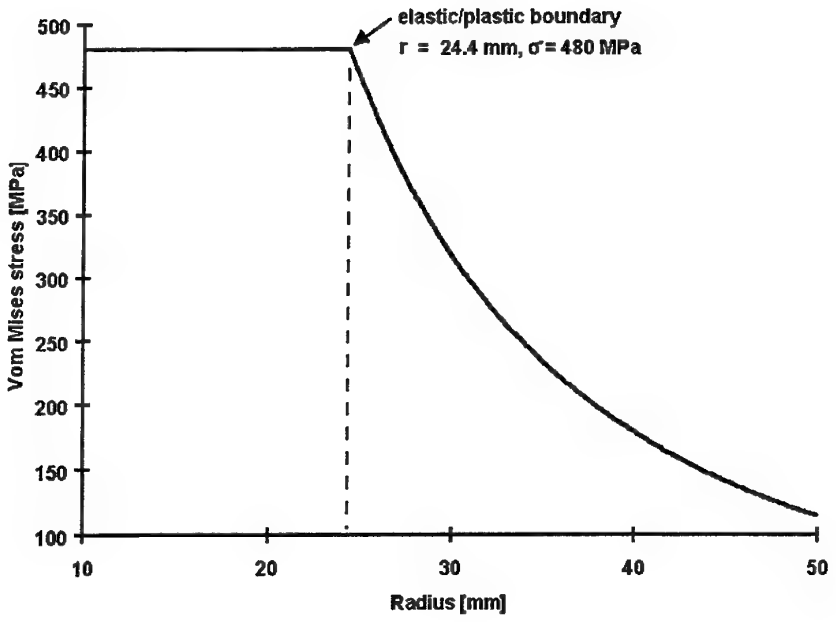

Figure 11: Von-Mises stress distribution as a function of radius showing location of elastic/plastic boundary determined from finite element analysis at 4% interference

The analysis of Jost [5] can be used to calculate the location of the elastic-plastic boundary (c). For the given interference level of 4%, the value of c is determined by iteration from Equation (3) where

$$\lambda \frac{E}{\sigma_0} = \frac{1}{\sqrt{3}} \left\{ \left(1+\upsilon_p\right)\left(\frac{c}{a}\right)^2 \left[1+\left(1-2\upsilon_p\right)\left(\frac{c}{b}\right)^2 \right] + \left(1+\nu_m\right)\left(1-2\nu_m\right) g \left[2\ln\left(\frac{c}{a}\right) + 1 - \left(\frac{c}{b}\right)^2 \right] \right\} \quad (3)$$

Use of this equation yields a prediction for c of 26.36 mm, which compares favourably with the value obtained using finite element analysis of 24.4 mm as shown in Figure 11. Since the closed form solutions [5] are based on a deformation theory of plasticity, and the finite element analyses use incremental plasticity, some discrepancy between the results is to be expected.

4.3 Elastic-Perfectly Plastic Analysis of a 1.5% Cold Expanded Steel Annulus With a Subsequent 0.5 % Steel Mandrel Interference Fitting

In this case the finite element mesh (Figure 3) consisted of 120 equal divisions to represent the mandrel and 400 to represent the annulus, as for the case discussed in Section 4.2. The geometric and material parameters used were as follows: b = 75 mm, a = 10.0 mm, $\nu_p = \nu_m = 0.3$, g = 1, $\sigma_0 = 1200$ MPa and $E_p = E_m = 209$ GPa. To model the cold expansion, the constraint conditions were applied incrementally as follows: one increment of 0.54%, followed by two increments of 0.015%, six increments of 0.03% and ten increment of 0.075%. This resulted in a total cold expansion of 1.5%. Unloading from this level was with two increment at -0.075%, six increments at -0.15%, one increment of -0.075%, and then one increment of -0.015%. It is important to note that complete unloading was defined to occur when the radial stress at the edge of the hole was zero. The subsequent interference fitting level of 0.5% was achieved using six increments of 0.075%, one at 0.045% and one at 0.0045%.

4.3.1 Stresses at 1.5% Cold Expansion

The radial and hoop stress distributions in the annulus at the 1.5% cold expansion level, (i.e. before unloading) obtained from the finite element analysis, are shown in Figure 12.

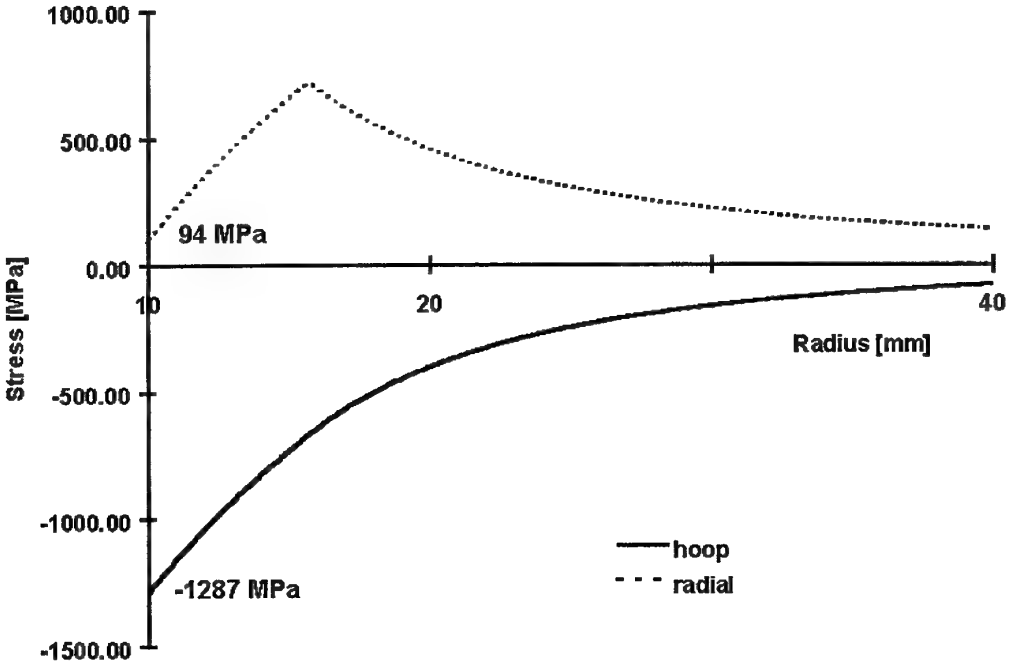

Figure 12: Finite element results for hoop and radial stress distributions in a steel annulus at 1.5% cold expansion

Predicted stresses in the plastic region [5] are given by equation (4), A comparison between the theoretical predictions and finite element results at the hole edge are given in Table 1, showing good agreement.

$$\sigma_r = \frac{\sigma_0}{\sqrt{3}}\left[2\ln\frac{r}{c} - 1 + \left(\frac{c}{b}\right)^2\right]$$

$$\sigma_\theta = \frac{\sigma_0}{\sqrt{3}}\left[2\ln\frac{r}{c} + 1 + \left(\frac{c}{b}\right)^2\right] \quad (4)$$

Table 1: Finite element and theoretical stresses at the hole edge for a steel annulus at 1.5% cold expansion

Component	Theory [5] (MPa)	Finite element (MPa)
σ_r	-1337	-1287
σ_θ	48	94

Figure 13 shows the finite element results for the von Mises stress distribution as a function of radial position through the annulus. This indicates an elastic-plastic boundary at c = 15.69 mm, as compared to a value of c = 16.30 mm predicted from equation (3).

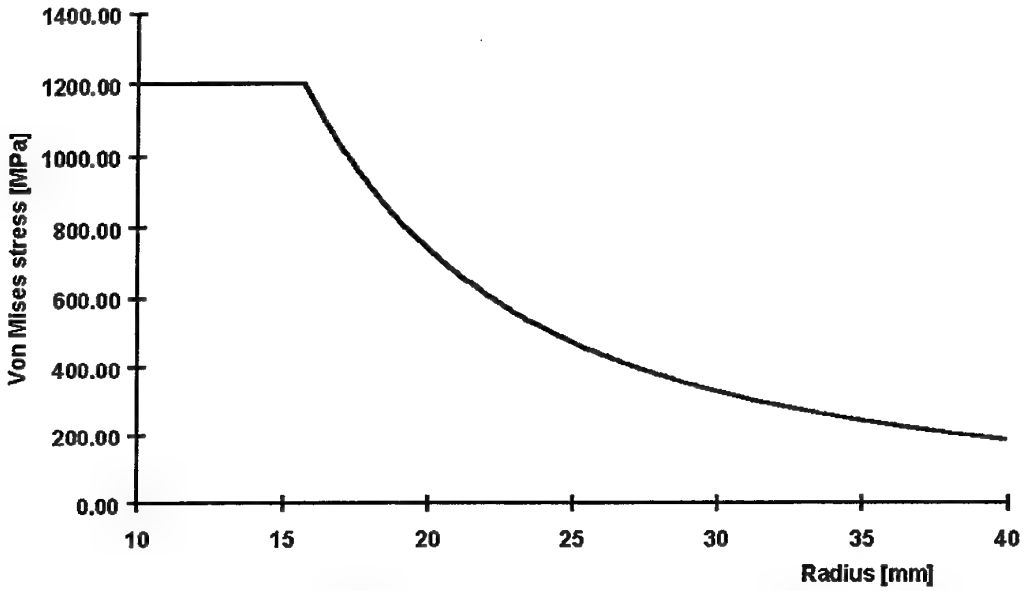

Figure 13: Finite element results for the von-Mises stress distribution through a steel annulus showing location of elastic-plastic boundary at 1.5% cold expansion.

4.3.2 Stresses After Removal of 1.5% Cold Expansion

Figure 14 shows the finite element results for the radial, hoop and von Mises stress distributions in the annulus at the completion of the cold expansion process. The magnitude of the residual compressive hoop stress is a maximum at the hole edge, and the material there is just below the incipient re-yield point.

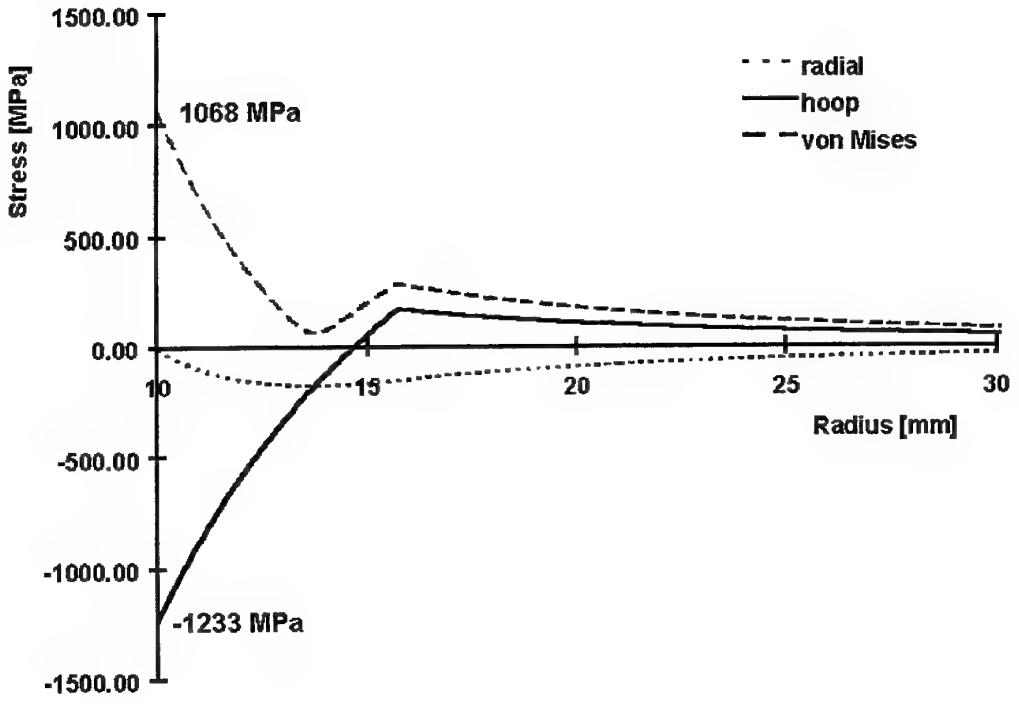

Figure 14: Finite element stress results for a steel annulus after 1.5% cold expansion then removal

From Reference 5 theoretical stresses in the plastic region at this condition (with no reyielding upon mandrel removal) are given by equation (5). A comparison between theoretical predictions and finite element results at the hole edge is given in Table 2, showing good agreement. It is important to note that the residual radial deformation after the removal of cold expansion is 0.0366 mm, or 0.366% of the initial hole radius.

$$\sigma_r^{CE} = \frac{\sigma_0}{\sqrt{3}}\left\{\left[2\ln\left(\frac{r}{c}\right) - 1 + \left(\frac{c}{b}\right)^2\right] + \alpha\frac{\left(\frac{a}{r}\right)^2 - \left(\frac{a}{b}\right)^2}{1-\left(\frac{a}{b}\right)^2}\right\}$$

$$\sigma_\theta^{CE} = \frac{\sigma_0}{\sqrt{3}}\left\{\left[2\ln\left(\frac{r}{c}\right) + 1 + \left(\frac{c}{b}\right)^2\right] - \alpha\frac{\left(\frac{a}{r}\right)^2 + \left(\frac{a}{b}\right)^2}{1-\left(\frac{a}{b}\right)^2}\right\} \quad (5)$$

$$\text{where } \alpha = 2\ln\left(\frac{c}{a}\right) + 1 - \left(\frac{c}{b}\right)^2$$

Table 2: Finite element and theoretical stresses at the hole edge after unloading from a 1.5% cold expansion level

Component	Theory [4] (MPa)	Finite element (MPa)
σ_r	0	-6
σ_θ	-1338	-1233

4.3.3 Stress History for 1.5% Cold Expansion and Subsequent 0.5% Interference Fitting

Figure 15 shows the variation of hoop, radial and von-mises stresses at the edge of the hole, as a function of the stage (i.e. time) in the cold expansion process and the subsequent interference fitting. The units on the horizontal axis represents a fictitious time scale, where each time interval corresponds to an increment in the finite element analysis. Since the analysis increments were non-uniform, it is a non-linear scale. The elastic-perfectly plastic response of the material can be clearly seen by inspection of the von Mises stress response. During the unloading phase of the cold expansion process, the material response is elastic, with the von Mises stress not being sufficient in magnitude to achieve re-yielding. It can be seen that the insertion of the interference fit mandrel induces only elastic deformations in the plate.

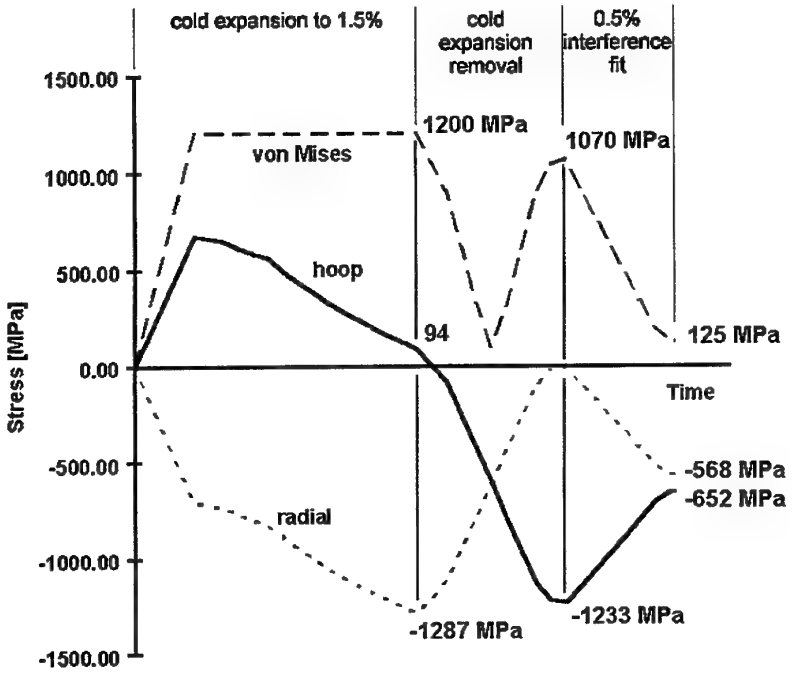

Figure 15 : Finite element stress history at the hole edge of the steel annulus, for cold expansion to 1.5%, followed by 0.5% interference fitting.

The closed-form solution to this problem [4] is given in equation (6).

$$\sigma_r^{CE} = \sigma_r^{CE} - \frac{\lambda E}{D}\left[\left(\frac{a}{r}\right)^2 - \left(\frac{a}{b}\right)^2\right]$$

$$\sigma_\theta^{CE} = \sigma_\theta^{CE} + \frac{\lambda E}{D}\left[\left(\frac{a}{r}\right)^2 + \left(\frac{a}{b}\right)^2\right] \qquad (6)$$

Here the first term in each equation is due to cold expansion (equation (5)). The second term is due to interference only and is assumed to vary linearly with increasing interference level. The results from the finite element analysis and those predicted from theory [4] are presented in Table 3, showing good agreement.

Table 3: Finite element and theoretical stresses at the hole edge for an annulus after 1.5% cold expansion and subsequent interference fitting to 0.5%

Component	Theory[4] (MPa)	Finite element (MPa)
σ_r	-567 MPa	-568 MPa
σ_θ	-750 MPa	-652 MPa

5. Analysis of Enhanced Circular Hole in a Large Rectangular Plate Under Representative F-111C Loading Conditions

Following the successful analyses presented in Section 4 on various benchmark problems, more complex cases representative of the F-111C wing pivot fitting material constitutive behaviour and loading conditions were undertaken. For example, results of analyses undertaken assuming a strain hardening response of D6ac steel are presented (Figure 9). Also, loads representative of those experienced by the stiffener containing FFVH13, are applied, namely: (i) Cold Proof Load Test (CPLT) and (ii) a sample remote spectrum loading of ± 200 MPa.

The plastic finite element analyses described in this Section are for a large rectangular flat steel plate which is 300 mm long, 150 mm wide and with a 10 mm radius circular hole. For all cases the finite element mesh was similar to that shown in Figure 5, and unless otherwise noted the cold expansion level was 1.5% and the subsequent interference fit level was 0.5%, and the no-slip constraint conditions were used (Equations 1 and 2). The results are presented at the critical location, i.e. at θ=0° (Figure 4), for both slip and no-slip cases. The cases considered can be summarised as follows:

Unenhanced

1. Remote loading only for plate with an open circular hole assuming strain hardening material properties.

Enhanced

1. Cold expansion and subsequent interference fitting assuming elastic-perfectly plastic material properties for the plate.
2. Cold expansion, subsequent interference fitting and remote loading assuming elastic-perfectly plastic material properties for the plate.
3. Cold expansion, subsequent interference fitting and remote loading assuming strain hardening material properties for the plate.
4. Cold expansion, subsequent interference fitting and remote loading assuming strain hardening material properties for the plate, with slip allowed to occur during the interference fitting process and under the remote loading.
5. Interference fitting and remote loading for the plate with strain hardening material properties, for both no-slip and slip allowed cases.

5.1 Unenhanced Hole With Remote Loading Assuming Strain Hardening Material

For this analysis strain hardening material properties were used to permit direct comparison with the results of the enhanced analyses presented in Sections 5.4,5.5 & 5.6. The stress results for the edge of the open hole at θ=0° are given in Figure 16.

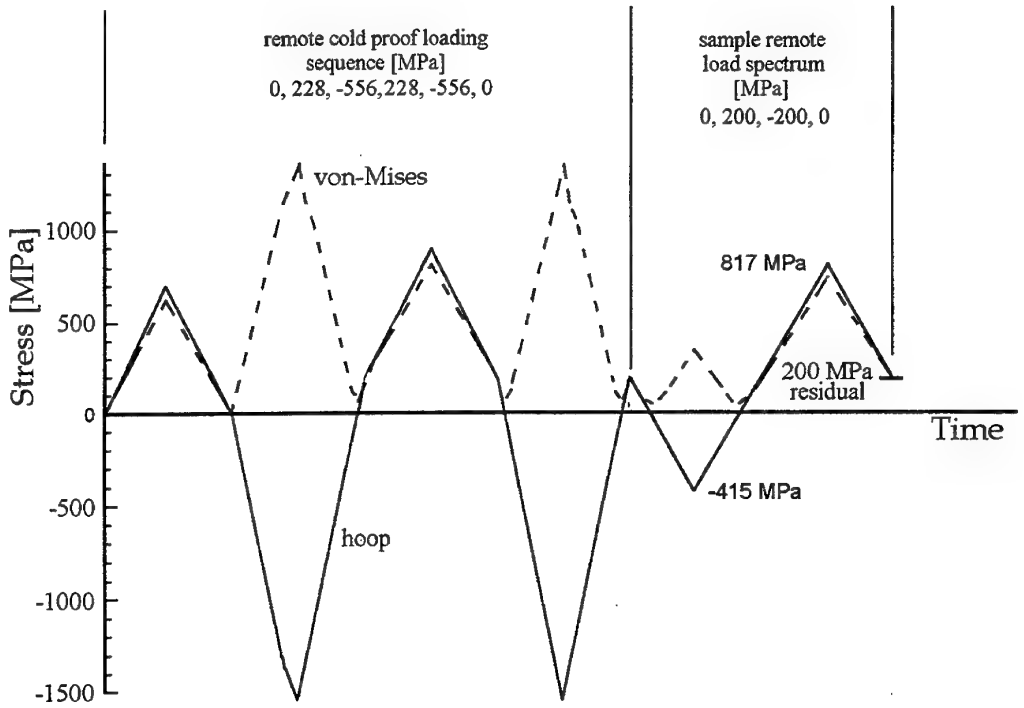

Figure 16: Finite element stress history at the hole edge, θ=0°, for the unenhanced rectangular plate of strain hardening material with CPLT and then remote spectrum loading

As can be seen from Figure 16, residual tensile stresses due to the CPLT equivalent loading occur, and this is consistent with experimental results obtained from strain surveys conducted during F-111C wing loading tests. The stress response is elastic for the application and removal of the remote tensile loading of 228 MPa. However the high remote compressive loading to -556 MPa causes material yielding, and upon its removal, a residual tensile hoop stress of 200 MPa is induced. The stress response due to the subsequent sample remote loading is linear, and hence a residual hoop stress of 200 MPa exists at the end of this loading. Since the hole is unfilled, the cyclic stress concentration factor due to remote loading is 3.1.

5.2 Cold Expanded and Interference Fitted Hole Assuming Elastic-Perfectly Plastic Material

Here cold expansion was modelled with one increment of 0.21% interference followed by eight increments of 0.03% and fourteen increments of 0.075%. Cold expansion unloading (removal) was achieved with fourteen increments of -0.075% and one increment of 0.09% to a achieve a condition of zero radial stress at the critical location. Interference fitting of the mandrel was achieved with 10 increments of 0.05%.

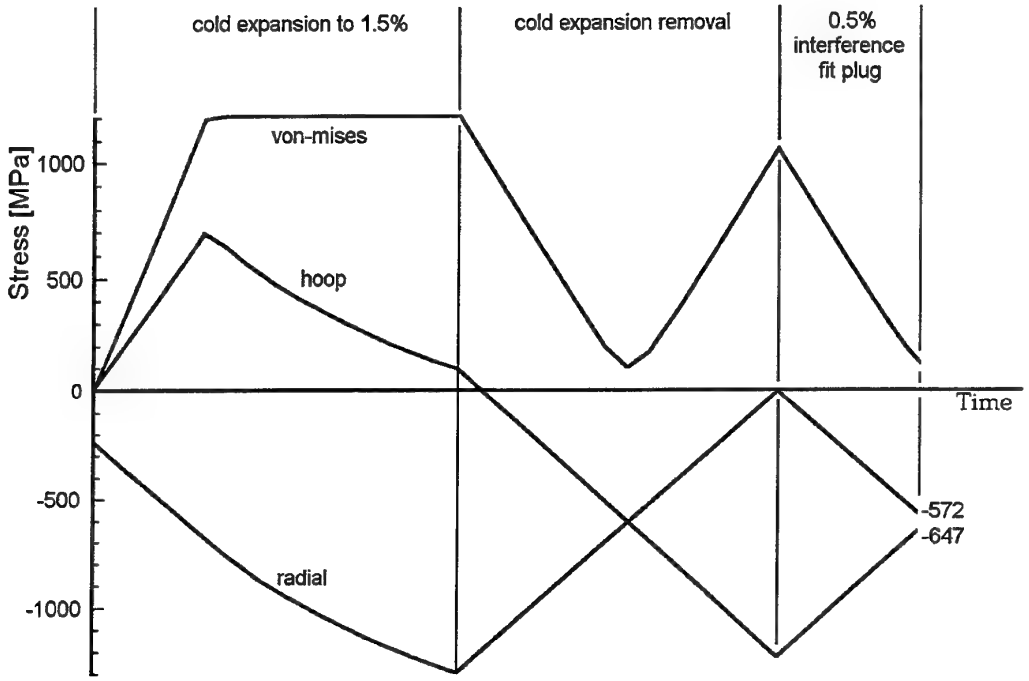

Figure 17: Finite element stress history at the hole edge, θ=0°, for the enhanced rectangular plate of elastic-perfectly plastic material with cold expanded to 1.5%, followed by 0.5% interference fitting

The results presented in Figure 17 for this case serve as a useful guide to understanding clearly the mechanism of stress response due to the cold expansion and interference processes. During cold expansion, the compressive radial stress increases in magnitude with increasing interference level. As the steel was modelled here as an elastic-perfectly plastic material, the von Mises response curve is flat after the yield point is reached. Hence once yielding has occurred, the hoop stress must reduce with the increase in interference (i.e. increasing magnitude of compressive radial stress). On removal of the cold expansion, such that the radial stress is zero, there is a resulting residual hoop stress of -1227 MPa. The subsequent application of the interference mandrel then results in residual compressive radial stress, and a reduction in the

magnitude of the residual compressive hoop stress. The finite element results from this analysis of the large plate can be compared directly with the those obtained for the annulus shown in Figure 15, along with the corresponding analytical predictions. For comparison purposes, the results at different stages in the enhancement process history are summarised in Tables 4, 5 & 6, for the location $\theta=0°$ at the hole edge. The residual expansion of the hole boundary, after completion of the cold expansion process, was found to be 0.035740 mm ± 0.000121 mm.

Table 4: Stresses at the hole edge at 1.5% cold expansion level

Component	Annulus (Theory [1])	Annulus (Finite element)	Plate (Finite element)
σ_r	-1337 MPa	-1287 MPa	-1212 MPa
σ_θ	48 MPa	94 MPa	172 MPa

Table 5: Stresses at the hole edge after removal of 1.5% cold expansion level

Component	Annulus (Theory[1])	Annulus (Finite element)	Plate (Finite element)
σ_r	0	-6 MPa	0
σ_θ	-1338 MPa	-1233 MPa	-1227 MPa

Table 6: Stresses at the hole edge after 1.5% cold expansion and subsequent interference fitting to 0.5%

Component	Annulus (Theory [1])	Annulus (Finite Element)	Plate (Finite Element)
σ_r	-567 MPa	-568 MPa	-572 MPa
σ_θ	-750 MPa	-652 MPa	-647 MPa

The differences between analytical and finite element results for the annulus were discussed in Section 4.2. From the results given in Tables 4 to 6, it can be concluded that the finite element modelling methods used for the analysis of the large rectangular large plate are sound.

5.3 Cold Expanded and Interference Fitted Hole with Remote Loading Assuming Elastic-Perfectly Plastic Material

This analysis case is the same as that presented in Section 5.2, except that uniaxial remote loading is now applied to the plate after the completion of the interference fitting. The remote loading was chosen to represent the CPLT followed by a sample spectrum loading. One objective for this analysis is to provide results that may be compared with those obtained for the case assuming strain hardening material response, which are given in the next section. The results for the analysis are shown in Figure 18.

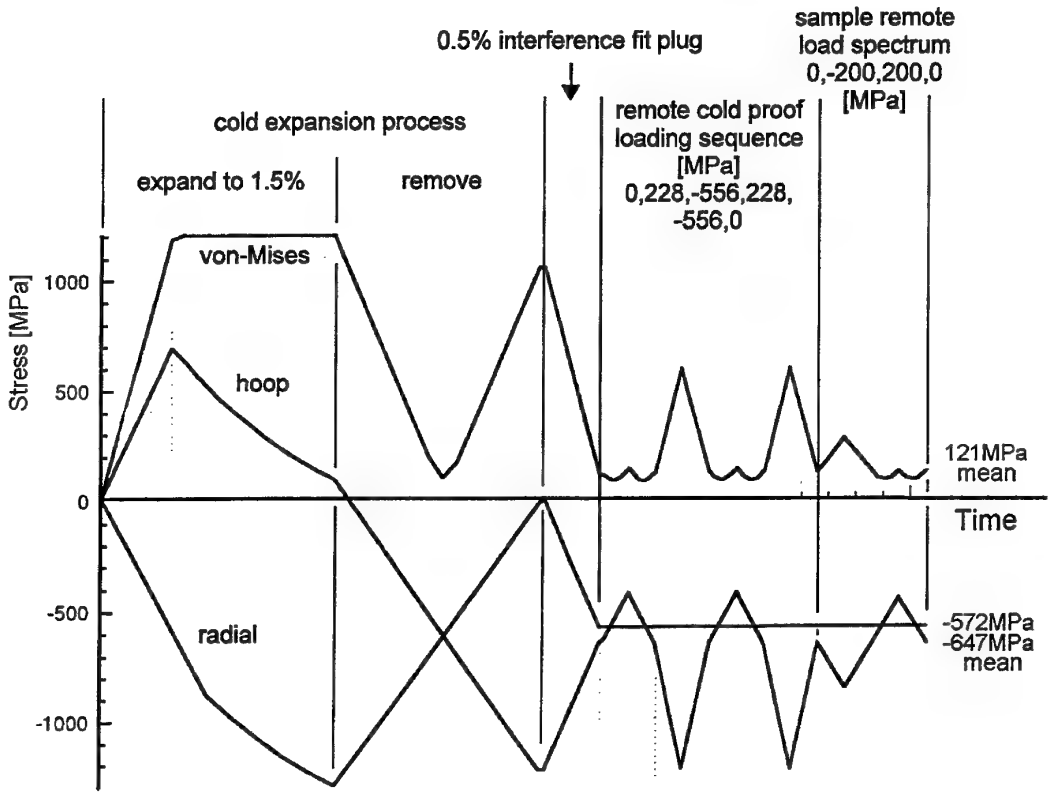

Figure 18: Finite element stress history at the hole edge, θ=0°, for the enhanced rectangular plate of elastic-perfectly plastic material, with cold expanded to 1.5%, followed by 0.5% interference, CPLT and then remote spectrum loading (no slip)

Here it can be seen that during the sample remote loading of ±200 MPa, the mean stress is compressive at -647 MPa, and the cyclic stress peaks are -447 MPa and -847 MPa. This gives a cyclic stress concentration factor of unity. It can be seen that the fatigue-damaging effect of a high mean stress coupled with a large cyclic stress concentration, as previously existed for the open hole (Figure 16) case, has been greatly

reduced. Another point of interest demonstrated by this analysis is the constant radial stress value during the application of remote loading. This is because the interference fit mandrel installation has effectively filled the hole, so then the remote uniaxial loading does not create any stress in the direction perpendicular to its application.

5.4 Cold Expanded and Interference Fitted Hole with Remote Loading Assuming Strain Hardening Material

The use of strain hardening material properties gives a more realistic estimate of stresses during the cold expansion and interference fit process. The magnitude of the residual stress at the edge of the hole, and the size of the compressive region, are significantly influenced by the work hardening behaviour of the material. Typically the use of strain hardening material causes the size of the compressive residual stress region to be larger for a given level of cold-expansion, as compared to the elastic-perfectly plastic case. The results obtained are given in Figure 19, and can be compared directly with those obtained for an elastic-perfectly plastic material as given in Figure 18.

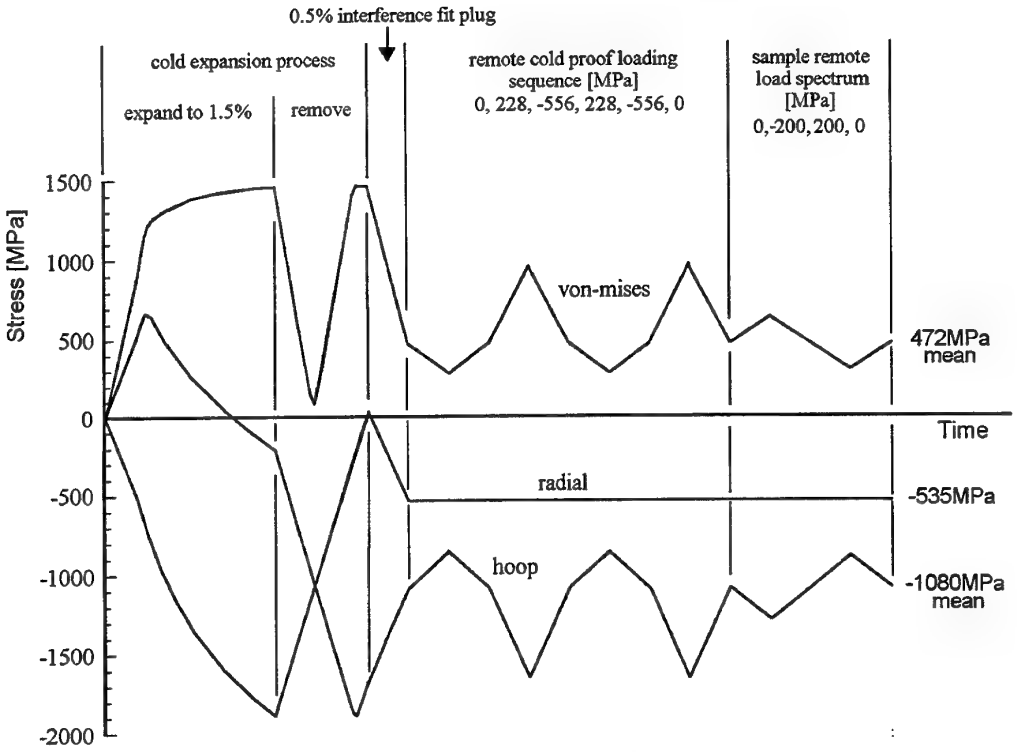

Figure 19: Finite element stress history at the hole edge, θ=0°, for the enhanced rectangular plate of strain hardening material, with cold expanded to 1.5%, followed by 0.5% interference, CPLT and then remote spectrum loading (no slip)

It is seen from Figure 19 that due to the strain hardening material response, the compressive residual hoop stress (after the CPLT) is much lower in magnitude, as compared to the elastic-perfectly plastic material case, having changed from -647 MPa to -1080 MPa. The radial stress remains essentially the same as for the elastic-perfectly plastic material case because the material stress response during the interference fit process is elastic (the radial stress having started from zero). The linear response subsequent to interference fitting indicates that the cyclic stress concentration factor remains the same as for the elastic-perfectly plastic material case, i.e. unity. The residual deformation around the hole after the cold expansion process was found to be 0.030122 mm ± 0.000075 mm, which is slightly less than the value of 0.035740 mm obtained for the plate with elastic-perfectly plastic material in Section 5.2.

5.5 Cold Expanded and Interference Fitted Hole with Remote Loading Assuming Strain Hardening Material and Slip Allowed

In practice, the interference fit mandrel can potentially slip during the application of external loading, if the loading is high enough. To investigate the effect of slip on plate stresses, analyses were performed for the case where there is no displacement constraint at the mandrel/plate interface in the local hoop direction (see Equation (2) and Figure 7). The results for this analysis are shown in Figure 20.

Subsequent to the CPLT, the mean hoop stresses for the slip allowed case remain essentially the same as for the no-slip case as given in Section 5.3. For example the value of mean hoop stress has only changed from -1080 MPa for the no-slip case to -1071 MPa for the slip allowed case. However, it is seen that by allowing slip to occur, the cyclic stress concentration at the hole edge is increased as compared to the no-slip case. For example, the cyclic stress peaks are -720 MPa and -1429 MPa, giving an increase in the cyclic stress concentration factor from 1.0 to 1.79, as compared to the no-slip case. There is still however, a major reduction in the cyclic stress range as compared to those for the open hole case (Figure 16), and significantly, the hoop stresses never become tensile during the remote loading.

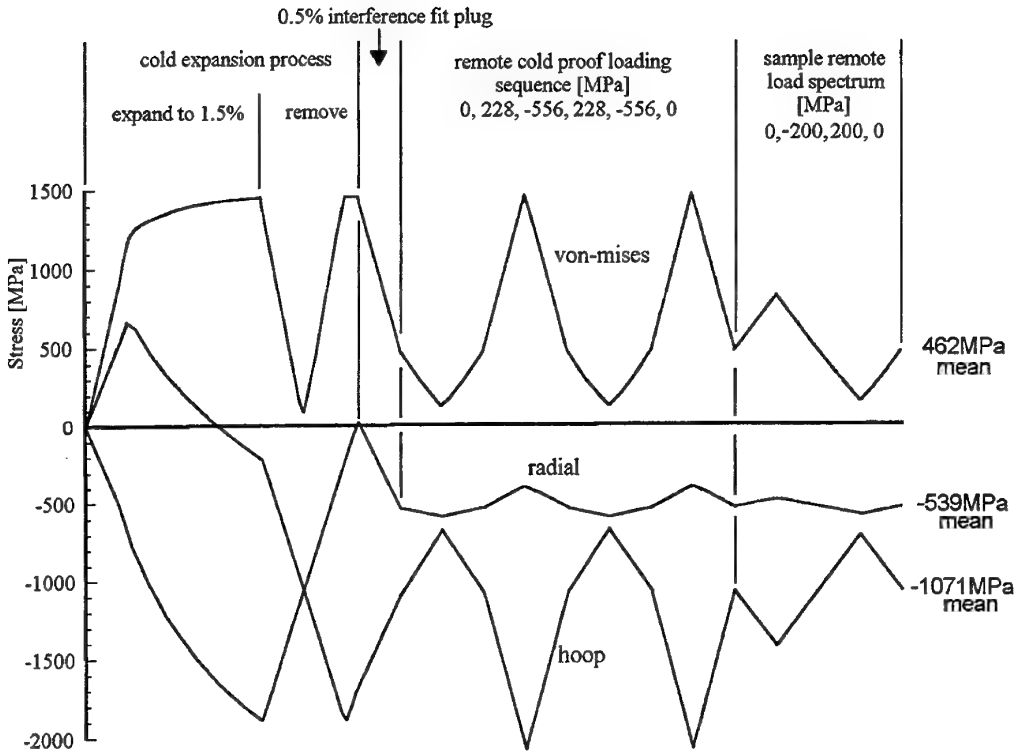

Figure 20: Finite element stress history at the hole edge, θ=0°, for the enhanced rectangular plate of strain hardening material, with cold expanded to 1.5%, followed by 0.5% interference, CPLT and then remote spectrum loading with slip allowed

5.6 Interference Fitted Hole With Remote Loading Assuming Strain Hardening Material

The analysis results for this enhancement case, assuming no-slip, are shown in Figure 21. It can be seen that the stress response is elastic for mandrel insertion and the subsequent remote loading. Clearly the mean stresses are relatively high, however the cyclic stress concentration has been reduced to unity.

The corresponding results for the slip allowed case are presented in Figure 22.

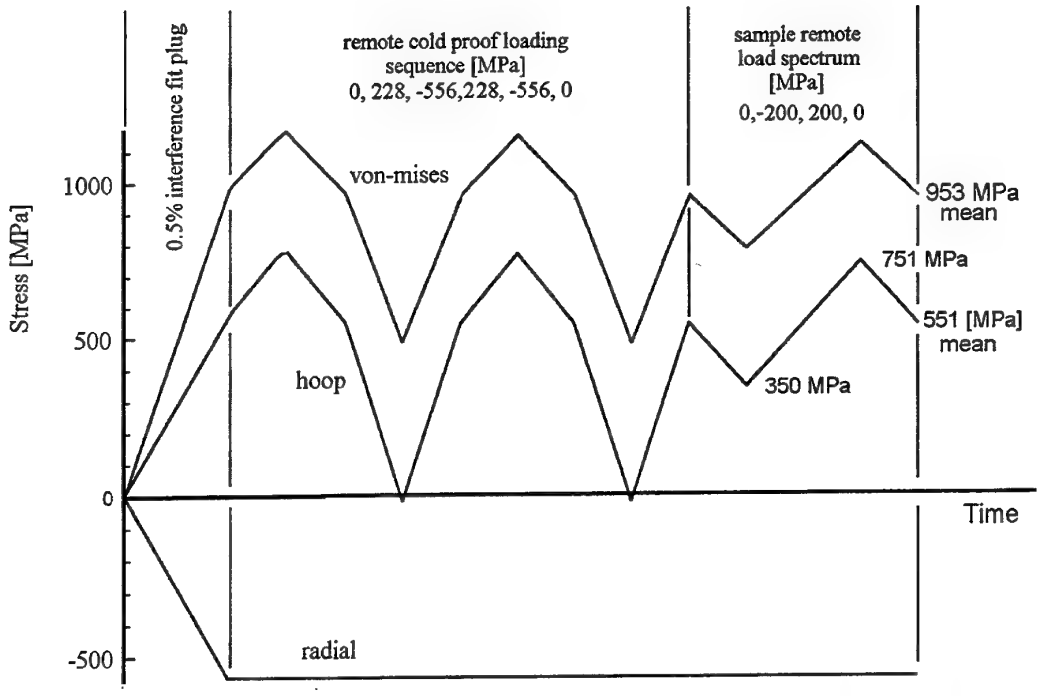

Figure 21: Finite element stress history at the hole edge, θ=0°, for the enhanced rectangular plate of strain hardening material, 0.5% interference fitting, CPLT and then remote spectrum loading with no slip

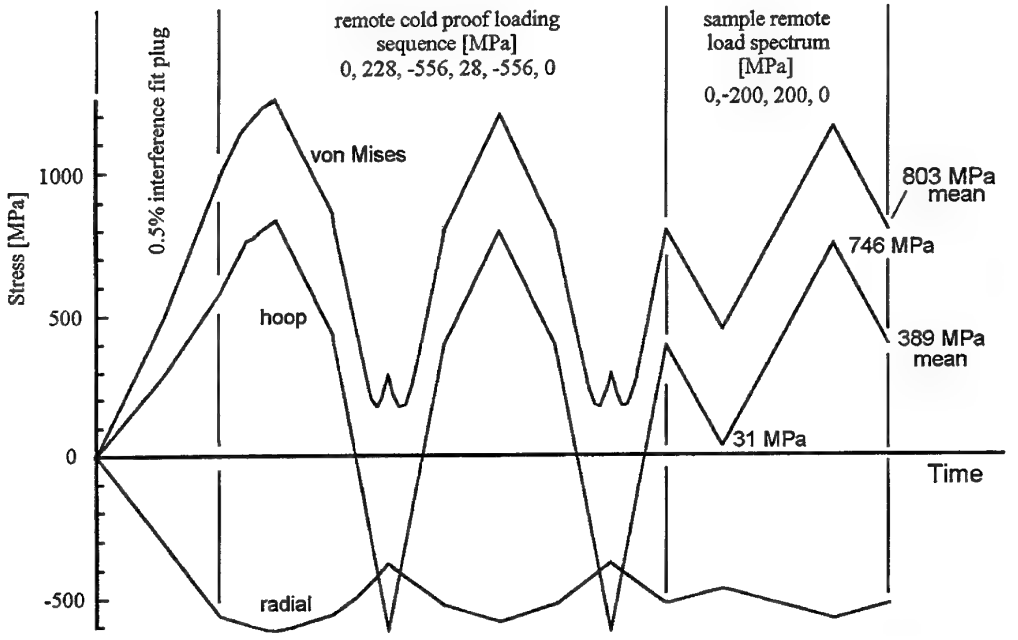

Figure 22: Finite element stress history at the hole edge, θ=0°, for the enhanced rectangular plate of strain hardening material, 0.5% interference fitting, CPLT and then remote spectrum loading with slip allowed

Here we see, as found in Section 5.5, the main effect of slippage between mandrel and plate is to increase the cyclic stress concentration factor from unity for the no-slip case to 1.79 for the slip allowed case.

5.7 Summary of Hoop Stress Responses Due to Sample Remote Loading

In the previous Sections, 5.1 to 5.6, the results for von-Mises, hoop and radial stresses have been presented in detail for various enhancement cases. In the context of fatigue life extension, the quantities of key interest are the mean and hoop stress responses due to remote loading at the critical location, θ=0°. To allow for a convenient comparison of the effect of the various enhancement cases, these results are given in Table 7. It is immediately apparent that there is a very significant advantage in having combined cold-expansion with interference fitting, as opposed to interference fitting only.

Table 7: Mean and cyclic hoop stresses at the hole edge for various enhancement cases for a rectangular plate due to sample remote loading of +/- 200 MPa

Enhancement case and material constitutive response assumption	Mean hoop stress (MPa)	Cyclic hoop stresses (MPa)	Stress concentration
Open hole -(SHM)*	200	-415 to 817	3.1
No slip cases			
1.5 % CE with 0.5% IF - (EPPM)**	-647	-847 to -447	1.0
1.5 % CE with 0.5% IF - (SHM)	-1080	-1280 to -880	1.0
0.5% IF - (SHM)	551	350 to 751	1.0
Slip allowed cases			
1.5 % CE with 0.5% IF - (SHM)	-1071	-1429 to -720	1.79
0.5% IF - (SHM)	389	+31 to 746	1.79

* strain hardening material
** elastic-perfectly plastic material

6. Conclusions

This report presents the detailed stress responses for a large rectangular plate of D6ac material, subjected to the following: (a) enhancement by cold expansion and/or interference fitting, (b) representative cold proof test loading (CPLT), and (c) a sample spectrum loading. The stress responses were determined using elastic plastic finite element analysis methods assuming plane-strain conditions. For the case where there is no-slip at the mandrel/hole interface, and assuming strain hardening material constitutive response, (unless otherwise noted) the study indicates the following:

(i) Results derived from benchmark analyses, assuming elastic-perfectly plastic material response, compare well with analytical predictions, and consistent with the assumptions taken, provide confidence in the finite element procedures used.

(ii) For the unenhanced open hole, application of the CPLT results in a significant residual tensile hoop stress of 200 MPa, at the critical location on the hole edge. Hence during application of the remote loading, the mean stress was 200 MPa and the cyclic stress concentration factor was 3.1.

(iii) For all enhancement cases, the stress response during the sample remote loading subsequent to the CPLT was linear, with a cyclic stress concentration factor of unity.

(iv) For the combined cold expansion and interference fitting enhancement case, the assumption of strain hardening material properties as compared to elastically perfectly plastic properties, had no effect on the cyclic stress concentration factor. However as expected, using strain hardening properties resulted in a lower mean stress (i.e. -1080 MPa as compared to -647 MPa).

(v) Enhancement through combined cold expansion and interference fitting was a great deal better than interference fitting only. For the enhanced case with cold expansion of 1.5% followed by interference fitting of 0.5 %, there was a residual (compressive) hoop stress of -1080 MPa as compared to a residual (tensile) hoop stress of 350 MPa for the interference fitting only case.

(vi) For all enhancement cases the assumption of slip allowed, as compared to no-slip, led to significant increases in the cyclic stress concentration, i.e. from 1 to 1.79. There was however much less effect on the mean stress. Even for this highly conservative assumption, there was no tensile component of hoop stress during remote loading, for the combined cold expansion and interference fitting enhancement.

(vii) Overall enhancement through combined cold expansion with interference fitting is considered highly beneficial, with the favourable stresses generated not adversely affected by subsequent CPLT.

7. Acknowledgments

The authors wish to acknowledge the helpful comments given by Mr K. C. Watters, Dr L. F. R. Rose, Mr J. Paul, Mr P. Piperias, Dr G. Jost, and Dr N. Rajic.

8. References

1. **KEYS, R.H., MOLENT, L., GRAHAM, A.D.,** *F-111 wing pivot fitting finite element analysis of rework of fuel flow vent hole #13,* DSTO, ARL, Aircraft Structures Technical Memorandum 557, 1992.

2. **MANN, J.Y., and JOST, G.S.,** *Stress fields associated with interference-fitted and cold-expanded holes, with particular reference to the fatigue life enhancement of aircraft structural joints,* Metals Forum, Vol. 6, No. 1. 1983.

3. **BROEK, D.,** *The practical use of fracture mechanics,* Kluwer Academic Publishers, Dordrecht, 1989.

4. **JOST, G.S.,** *Stresses and strains in plain and cold worked annuli subjected to remote, interference or combined loading.* DSTO, ARL, Aircraft Structures Report 446, May 1992.

5. **JOST, G.S.,** *Stresses and strains in a cold-worked annulus,* DSTO, ARL, Aircraft Structures Report 434, September 1988.

6. **PIPERIAS, P. and HELLER, M.,** *Optimisation of stresses around holes using sleeve/bolt combinations,* Proceedings of the 5th Australian Aeronautical Conference, Melbourne pp. 309-315, 1993.

THIS PAGE INTENTIONALLY BLANK

Appendix A

Example PAFEC Input Data File for 1.5% Cold Expanded Annulus With Subsequent 0.5% Interference Fitting

```
C        FILE :  STSTSEGPS4.DAT
C
C        TITLE : INTERFERENCE FIT, ROUND HOLE,
C              STEEL PLATE AND STEEL PLUG,
C              2.5deg SEGMENT
C
C              Plug Outside Radius = 10.15 mm
C              Annulus Outside Rad = 100.0 mm
C              Annulus Inside Rad. = 10.0 mm
C              Annulus Material : Steel      E = 209E3
C              Plug Material    : Steel      E = 209E3
C
C              1.5% Cold expansion % 0.5% Interference fitting
C
CONTROL
FULL.CONTROL
PLANE.STRAIN
PHASE=1
PHASE=2
PHASE=4
PHASE=6
PHASE=7
PLASTICITY
PHASE=9
BASE=5555555
CONTROL.END
NODES
NODE.NUMBER          AXIS.NUM          X
1                    1                 0.0
2                    1                 0.65
3                    1                 10.15
4                    5                 0.65
5                    5                 10.15
6                    1                 10.0
7                    5                 10.0
8                    1                 100.0
9                    5                 100.0
10                   6                 10.15
11                   6                 10.0

NODES
C Nodes added for dummy plate
NODE.NUMBER          X                 Y
1000                 160               2
1001                 190               2
1002                 160               30
1003                 190               30
AXES
AXISN                RELA        TYPE        ANG1
```

```
5                       1           1           2.5
6                       1           1           1.25
C
LOCAL.DIRECTIONS
NODE                    LOCAL       PLANE       AXIS
4                       5           4           5
10                      6           4           6
C
PAFBLOCKS
TYPE=1
BLOCK     GROUP N1      N2     ELEMENT      PROP  TOPOLOGY
C  PLATE BLOCKS
1         1     1       2      36210        13    6 7 8 9 11
C  PLUG BLOCKS
2         2     1       3      36210        13    2 4 3 5 0 0 0 10
C  DUMMY BLOCK
3         3     1       1      36210        13    1000 1001 1002 1003
C
MESH
REFERENCE               SPACING.LIST
1                       1
2                       400
3                       120
C
PLATES.AND.SHELLS
PLATE.NUMBER            MATERIAL.NUMBER   THICKNESS
12                      13                5.0
13                      13                5.0
C
MATERIAL
MATERIAL.NUMBER         E                 NU
13                      209.0E3           0.3          C .....Steel
C
PLASTIC.MATERIAL
PLASTIC.MATERIAL        YIELD.CRITERION   UNIAXIAL.PROPS
13                      1                 13
C
UNIAXIAL.PROPS
UNIAXIAL                TYPE              PROPERTY
13                      1                 1200 ,   0
C
YIELDING.ELEMENTS
PLAS                    GROUP
13                      1         C   Plate
13                      2         C   Plug
13                      3         C   Dummy
C
C
CONVERGENCE
LOAD                    MAX.ITER    QUIT  TOLERANCE
1                       50          1     1
C
TOLERANCES
REFERENCE               TOL5
1                       0.00001
C
STATE.DETERMINATION
ALGOR                   TOL         PATH
2                       1E-5        1
```

```
C
INCREMENTAL
LOAD STEP
1       36 1 1 2 2 2 2 2 2 5 5 5 5 5 5 5 5 5
*       -5 -5 -10 -10 -10 -10 -10 -10 -5 -1
*        5 5 5 5 5 5 3 0.3
RESTRAINTS
NODE.NUMBER     PLANE       AXIS            DIRECTION
2               2           1               2
4               2           4               2
C
RESTRAINTS
NODE.NUMBER     PLANE       DIRECTION
1000            2           0
GENERALISED.CONSTRAINTS
DIRECTION=1
NODE            LIST
7               5,1,1    1002,1,1
6               3,1,1    1002,1,1
11              10,1,1   1002,1,1
C
DISPLACEMENTS.PRESCRIBED
NODE.NUMBER     DIRECTION           DISPLACEMENT.VALUE
1002            1                   0.15
C
END.OF.DATA
```

THIS PAGE INTENTIONALLY BLANK

Appendix B

Example PAFEC Input Data File for Rectangular plate with Cold Expanded and Interference Fitted Hole with Remote Loading

```
C        File : STSTAPS2.DAT
C
C        PAFEC 8.1 DATA FILE
C
C        TITLE :COLD WORKING 1.5% + INTERFERENCE FIT 0.5%
C        CPLT SPECTRUM + TYPICAL TENSION + TYPICAL COMPRESSION,
C        ROUND HOLE,
C        STEEL PLATE AND STEEL SLEEVE : E1/E2 = 1
C        PLANE STRESS ANALYSIS
C
C        Quarter plate model 75 mm x 150 mm
C        Hole radius = 10 mm
C        Mandrel radius = 10.1 mm
C        Plate and mandrel steel, E= 209E3
C
CONTROL
FULL.CONTROL
PLANE.STRAIN
PHASE=1
PHASE=2
PHASE=4
PHASE=6
PHASE=7
PLASTICITY
PHASE=9
BASE=5555555
STOP
CONTROL.END
NODES
NODE.NUMBER    X              Y
1              0              10.0
2              3.82683        9.23880
3              7.07107        7.07107
4              9.23880        3.82683
5              10.0           0.0
6              75.0           0.0
7              0.0            75.0
8              75.0           75.0
9              0.0            150.0
10             75.0           150.0
11             0.0            0.65
12             0.2487442      0.6005217
13             0.4596194      0.4596194
14             0.6005217      0.2487442
15             0.65           0.0
16             0.0            10.1
17             3.865103       9.331183
18             7.141778       7.141778
19             9.331183       3.865103
20             10.1           0
C
```

```
C
C Nodes added for dummy plate
1000            150             2
1001            170             2
1002            150             30
1003            170             30
C
C Nodes added for B.C.'s and Local Axes
21              0.784591        9.969174
22              1.564345        9.876884
23              2.334455        9.723701
24              3.090171        9.510568
25              4.539907        8.910068
26              5.224988        8.526404
27              5.877855        8.090173
28              6.494483        7.604064
214             7.604062        6.494483
215             8.090173        5.877855
216             8.526405        5.224987
217             8.910069        4.539907
218             9.510568        3.090171
219             9.723701        2.334454
220             9.876885        1.564345
221             9.969173        0.784591
585             0.792437        10.068865
586             1.579988        9.975653
587             2.357799        9.820937
588             3.121072        9.605671
589             4.585304        8.999166
590             5.277235        8.611666
591             5.936631        8.171072
592             6.559425        7.680100
696             7.680100        6.559425
697             8.171072        5.936631
698             8.611666        5.277235
699             8.999166        4.585304
700             9.605672        3.121072
701             9.820937        2.357798
702             9.975653        1.579988
703             10.068865       0.792438
C
C
AXES
RELA=     1.0
TYPE=     1
ANG2=     0.0
ANG3=     0.0
NODE            AXIS            ANG1
2               12              67.5000
3               13              45.0000
4               14              22.5000
5               15              0.0000E+00
21              16              85.5000
22              17              81.0000
23              18              76.5000
24              19              72.0000
25              20              63.0000
26              21              58.5000
27              22              54.0000
```

```
28              23              49.5000
214             24              40.5000
215             25              36.0000
216             26              31.5000
217             27              27.0000
218             28              18.0000
219             29              13.5000
220             30              9.00000
221             31              4.50000
C
LOCAL.DIRECTIONS
PLAN=      0
NODE            LOCAL           AXIS
2               12              12
3               13              13
4               14              14
5               15              15
21              16              16
22              17              17
23              18              18
24              19              19
25              20              20
26              21              21
27              22              22
28              23              23
214             24              24
215             25              25
216             26              26
217             27              27
218             28              28
219             29              29
220             30              30
221             31              31
C
LOCAL.DIRECTIONS
PLAN=      1
NODE            LOCAL           AXIS
17              12              12
18              13              13
19              14              14
20              15              15
585             16              16
586             17              17
587             18              18
588             19              19
589             20              20
590             21              21
591             22              22
592             23              23
696             24              24
697             25              25
698             26              26
699             27              27
700             28              28
701             29              29
702             30              30
703             31              31
PAFBLOCKS
TYPE=1
```

```
BLOCK    GROUP N1    N2    ELEMENT     PROP  TOPOLOGY
C  PLATE BLOCKS
1        1     1     5     36210       12    1 3 7 8 2
2        1     2     6     36210       12    3 5 8 6 4
3        1     3     7     36210       12    7 8 9 10
C  SLEEVE BLOCKS
4        2     1     8     36210       12    11 13 16 18 12 0 0 17
5        2     1     8     36210       12    13 15 18 20 14 0 0 19
C  DUMMY BLOCK
7        3     1     1     36210       12    1000 1001 1002 1003
C
MESH
REFERENCE      SPACING.LIST
1              5
2              5
3              5
5              0.025 0.025 0.025 0.05 0.05 0.05 0.1 0.1 0.1 0.25
*              0.5 0.5 0.75 1.25 1.5 1.5 2
6              0.025 0.025 0.025 0.05 0.05 0.05 0.1 0.1 0.1 0.25
*              0.5 0.5 0.75 1.25 1.5 1.5 2
7              5
8              1 1 1 1 1 .75 .4
C
MATERIAL
MATERIAL.NUMBER      E           NU
C Steel Sleeve
12                   209.0E3     0.3      C Steel Sleeve
C
RESTRAINTS
NODE.NUMBER          PLANE       DIRECTION
1                    1           1
5                    2           2
C
RESTRAINTS
NODE.NUMBER          PLANE       DIRECTION
1000                 2           0
GENERALISED.CONSTRAINTS
DIRECTION=2
NODE                 LIST
1                    16,2,1      1002,1,1
GENERALISED.CONSTRAINTS
DIRECTION=1
NODE                 LIST
2                    17,1,1      1002,1,1
3                    18,1,1      1002,1,1
4                    19,1,1      1002,1,1
5                    20,1,1      1002,1,1
21                   585,1,1     1002,1,1
22                   586,1,1     1002,1,1
23                   587,1,1     1002,1,1
24                   588,1,1     1002,1,1
25                   589,1,1     1002,1,1
26                   590,1,1     1002,1,1
27                   591,1,1     1002,1,1
28                   592,1,1     1002,1,1
214                  696,1,1     1002,1,1
215                  697,1,1     1002,1,1
216                  698,1,1     1002,1,1
217                  699,1,1     1002,1,1
```

```
218                     700,1,1       1002,1,1
219                     701,1,1       1002,1,1
220                     702,1,1       1002,1,1
221                     703,1,1       1002,1,1
C
GENERALISED.CONSTRAINTS
DIRECTION=2
NODE                    LIST
2                       17,2,1
3                       18,2,1
4                       19,2,1
21                      585,2,1
22                      586,2,1
23                      587,2,1
24                      588,2,1
25                      589,2,1
26                      590,2,1
27                      591,2,1
28                      592,2,1
214                     696,2,1
215                     697,2,1
216                     698,2,1
217                     699,2,1
218                     700,2,1
219                     701,2,1
220                     702,2,1
221                     703,2,1
C
PLATES.AND.SHELLS
PLATE.NUMBER            MATERIAL.NUMBER    THICKNESS
12                      12                 5.0
C
DISPLACEMENTS.PRESCRIBED
LOAD.CASE=1
NODE.NUMBER             DIRECTION          DISPLACEMENT.VALUE
1002                    1                  0.15
C
DISPLACEMENTS.PRESCRIBED
LOAD.CASE=2
NODE.NUMBER             DIRECTION          DISPLACEMENT.VALUE
1002                    1                  0.05
C
DISPLACEMENTS.PRESCRIBED
LOAD.CASE=3
NODE.NUMBER             DIRECTION          DISPLACEMENT.VALUE
1002                    1                  0.0
C
SURFACE.FOR.PRESSURE
LOAD.CASE=3
PRESSURE.VALUE          NODE               PLANE
 -228                   9                  2
C
DISPLACEMENTS.PRESCRIBED
LOAD.CASE=4
NODE.NUMBER             DIRECTION          DISPLACEMENT.VALUE
1002                    1                  0.0
C
SURFACE.FOR.PRESSURE
LOAD.CASE=4
```

```
PRESSURE.VALUE        NODE              PLANE
 565                  9                 2
C
DISPLACEMENTS.PRESCRIBED
LOAD.CASE=5
NODE.NUMBER           DIRECTION         DISPLACEMENT.VALUE
1002                  1                 0.0
C
SURFACE.FOR.PRESSURE
LOAD.CASE=5
PRESSURE.VALUE        NODE              PLANE
 -228                 9                 2
C
DISPLACEMENTS.PRESCRIBED
LOAD.CASE=6
NODE.NUMBER           DIRECTION         DISPLACEMENT.VALUE
1002                  1                 0.0
C
SURFACE.FOR.PRESSURE
LOAD.CASE=6
PRESSURE.VALUE        NODE              PLANE
 565                  9                 2
C
DISPLACEMENTS.PRESCRIBED
LOAD.CASE=7
NODE.NUMBER           DIRECTION         DISPLACEMENT.VALUE
1002                  1                 0.0
C
SURFACE.FOR.PRESSURE
LOAD.CASE=7
PRESSURE.VALUE        NODE              PLANE
 200                  9                 2
C
DISPLACEMENTS.PRESCRIBED
LOAD.CASE=8
NODE.NUMBER           DIRECTION         DISPLACEMENT.VALUE
1002                  1                 0.0
C
SURFACE.FOR.PRESSURE
LOAD.CASE=8
PRESSURE.VALUE        NODE              PLANE
 -200                 9                 2
C
PLASTIC.MATERIAL
PLASTIC.MATERIAL      YIELD.CRITERION   UNIAXIAL.PROPS
13                    1                 13
C
UNIAXIAL.PROPS
UNIAXIAL              TYPE              PROPERTY
13                    1                 1200 ,   0
C
YIELDING.ELEMENTS
PLAS                  GROUP
13                    1           C     Plate
13                    2           C     Plug
13                    3           C     Dummy
C
C
CONVERGENCE
```

```
LOAD                    MAX.ITER    QUIT        TOLERANCE
1                       25          1           1
C
TOLERANCES
REFERENCE               TOL5
1                       1.0
C
STATE.DETERMINATION
ALGOR                   TOL         PATH
2                       1E-3        1
C
INCREMENTAL
LOAD    STEP
C       Cold expansion to 1.5%
1       14 2 2 2 2 2 2 2 2 5 5 5 5 5 5 5 5 5 5 5 5 5  C 23 STEPS
C       Removal of load to zero radial stress
*       -5 -5 -5 -5 -5 -5 -5 -5 -5 -5 -5 -5 -5 -5 -6    C 15 STEPS
C       Interference fit to 0.5%
2       0 0 0 0 0 0 0 0 0 0 0 0 0 0 0 0 0 0 0 0 0
*       0 0 0 0 0 0 0 0 0 0 0 0 0 0 0 0 0 0 0
*       10 10 10 10 10 10 10 10 10 10
C       Remote tension to 228 MPa & back to zero
3       0 0 0 0 0 0 0 0 0 0 0 0 0 0 0 0 0 0 0 0 0
*       0 0 0 0 0 0 0 0 0 0 0 0 0 0 0 0 0 0 0
*       0 0 0 0 0 0 0 0 0 0 0
*       10 10 10 10 10 10 10 10 10 10
*       -10 -10 -10 -10 -10 -10 -10 -10 -10 -10
C       Remote compression to -565 MPa & back to zero
4       0 0 0 0 0 0 0 0 0 0 0 0 0 0 0 0 0 0 0 0 0
*       0 0 0 0 0 0 0 0 0 0 0 0 0 0 0 0 0 0 0
*       0 0 0 0 0 0 0 0 0 0 0
*       0 0 0 0 0 0 0 0 0 0 0
*       0 0 0 0 0 0 0 0 0 0 0
*       10 10 10 10 10 10 10 10 10 10
*       -10 -10 -10 -10 -10 -10 -10 -10 -10 -10
C       Remote tension to 228 MPa & back to zero
5       0 0 0 0 0 0 0 0 0 0 0 0 0 0 0 0 0 0 0 0 0
*       0 0 0 0 0 0 0 0 0 0 0 0 0 0 0 0 0 0 0
*       0 0 0 0 0 0 0 0 0 0 0
*       0 0 0 0 0 0 0 0 0 0 0
*       0 0 0 0 0 0 0 0 0 0 0
*       0 0 0 0 0 0 0 0 0 0 0
*       0 0 0 0 0 0 0 0 0 0 0
*       10 10 10 10 10 10 10 10 10 10
*       -10 -10 -10 -10 -10 -10 -10 -10 -10 -10
C       Remote compression to -565 MPa & back to zero
6       0 0 0 0 0 0 0 0 0 0 0 0 0 0 0 0 0 0 0 0 0
*       0 0 0 0 0 0 0 0 0 0 0 0 0 0 0 0 0 0 0
*       0 0 0 0 0 0 0 0 0 0 0
*       0 0 0 0 0 0 0 0 0 0 0
*       0 0 0 0 0 0 0 0 0 0 0
*       0 0 0 0 0 0 0 0 0 0 0
*       0 0 0 0 0 0 0 0 0 0 0
*       0 0 0 0 0 0 0 0 0 0 0
*       0 0 0 0 0 0 0 0 0 0 0
*       10 10 10 10 10 10 10 10 10 10
*       -10 -10 -10 -10 -10 -10 -10 -10 -10 -10
C       Remote compression to -200 MPa & back to zero
7       0 0 0 0 0 0 0 0 0 0 0 0 0 0 0 0 0 0 0 0 0
```

```
*       0 0 0 0 0 0 0 0 0 0 0 0 0 0 0 0 0 0
*       0 0 0 0 0 0 0 0 0 0
*       0 0 0 0 0 0 0 0 0 0
*       0 0 0 0 0 0 0 0 0 0
*       0 0 0 0 0 0 0 0 0 0
*       0 0 0 0 0 0 0 0 0 0
*       0 0 0 0 0 0 0 0 0 0
*       0 0 0 0 0 0 0 0 0 0
*       0 0 0 0 0 0 0 0 0 0
*       0 0 0 0 0 0 0 0 0 0
*       10 10 10 10 10 10 10 10 10 10
*       -10 -10 -10 -10 -10 -10 -10 -10 -10 -10
C       Remote tension to 200 MPa & back to zero
8       0 0 0 0 0 0 0 0 0 0 0 0 0 0 0 0 0 0 0 0
*       0 0 0 0 0 0 0 0 0 0 0 0 0 0 0 0 0 0 0 0
*       0 0 0 0 0 0 0 0 0 0
*       0 0 0 0 0 0 0 0 0 0
*       0 0 0 0 0 0 0 0 0 0
*       0 0 0 0 0 0 0 0 0 0
*       0 0 0 0 0 0 0 0 0 0
*       0 0 0 0 0 0 0 0 0 0
*       0 0 0 0 0 0 0 0 0 0
*       0 0 0 0 0 0 0 0 0 0
*       0 0 0 0 0 0 0 0 0 0
*       0 0 0 0 0 0 0 0 0 0
*       10 10 10 10 10 10 10 10 10 10
*       -10 -10 -10 -10 -10 -10 -10 -10 -10 -10
C
END.OF.DATA
```

DISTRIBUTION LIST

Stress Analysis of a Plate Containing a Round Hole with Combined Cold Expansion and Interference Fitting Under F-111C Representative Loading Conditions

R.B. Allan and M. Heller

AUSTRALIA

DEFENCE ORGANISATION

Task Sponsor AIR OIC ASI-LSA

S&T Program

Chief Defence Scientist
FAS Science Policy } shared copy
AS Science Corporate Management
Director General Science Policy Development
Counsellor Defence Science, London (Doc Data Sheet)
Counsellor Defence Science, Washington (Doc Data Sheet)
Scientific Adviser to MRDC Thailand (Doc Data Sheet)
Director General Scientific Advisers and Trials/Scientific Adviser Policy and Command (shared copy)
Navy Scientific Adviser (Doc Data Sheet and distribution list only)
Scientific Adviser - Army (Doc Data Sheet and distribution list only)
Air Force Scientific Adviser
Director Trials

Aeronautical and Maritime Research Laboratory

Director

Chief of Airframes and Engines Division
Research Leader Fracture Mechanics
Research Leader Structural Integrity
Reseach Leader Aerospace Composites
K. Watters
G. Clark
I. Anderson
L. Molent
D. Lombardo
P. Piperias
R.B. Allan (5 copies)
M. Heller (5 copies)

DSTO Library

Library Fishermens Bend
Library Maribyrnong
Library Salisbury (2 copies)
Australian Archives
Library, MOD, Pyrmont (Doc Data sheet only)

Forces Executive

Director General Force Development (Sea) (Doc Data Sheet only)
Director General Force Development (Land) (Doc Data Sheet only)

Army

ABCA Office, G-1-34, Russell Offices, Canberra (4 copies)

Air Force

OIC ATF ATS, RAAFSTT, WAGGA (2 copies)
CENG 501 Wing, Amberley

S&I Program

Defence Intelligence Organisation
Library, Defence Signals Directorate (Doc Data Sheet only)

B&M Program (libraries)

OIC TRS, Defence Regional Library, Canberra
Officer in Charge, Document Exchange Centre (DEC), 1 copy
*US Defence Technical Information Centre, 2 copies
*UK Defence Research Information Center, 2 copies
*Canada Defence Scientific Information Service, 1 copy
*NZ Defence Information Centre, 1 copy
National Library of Australia, 1 copy

UNIVERSITIES AND COLLEGES

Australian Defence Force Academy
Library
Head of Aerospace and Mechanical Engineering
Deakin University, Serials Section (M list), Deakin University Library, Geelong, 3217
Senior Librarian, Hargrave Library, Monash University
Librarian, Flinders University

OTHER ORGANISATIONS

NASA (Canberra)
AGPS

OUTSIDE AUSTRALIA

ABSTRACTING AND INFORMATION ORGANISATIONS

INSPEC: Acquisitions Section Institution of Electrical Engineers
Library, Chemical Abstracts Reference Service
Engineering Societies Library, US
Materials Information, Cambridge Scientific Abstracts, US
Documents Librarian, The Center for Research Libraries, US

INFORMATION EXCHANGE AGREEMENT PARTNERS

Acquisitions Unit, Science Reference and Information Service, UK
Library - Exchange Desk, National Institute of Standards and Technology, US
National Aerospace Laboratory, Japan
National Aerospace Laboratory, Netherlands

SPARES (10 copies)

Total number of copies: 75

DEFENCE SCIENCE AND TECHNOLOGY ORGANISATION
DOCUMENT CONTROL DATA

1. PRIVACY MARKING/CAVEAT (OF DOCUMENT)

2. TITLE

Stress Analysis of a Plate Containing a Round Hole with Combined Cold Expansion and Interference Fitting Under F-111C Representative Loading Conditions

3. SECURITY CLASSIFICATION (FOR UNCLASSIFIED REPORTS THAT ARE LIMITED RELEASE USE (L) NEXT TO DOCUMENT CLASSIFICATION)

Document	(U)
Title	(U)
Abstract	(U)

4. AUTHOR(S)

R.B. Allan and M. Heller

5. CORPORATE AUTHOR

Aeronautical and Maritime Research Laboratory
PO Box 4331
Melbourne Vic 3001

6a. DSTO NUMBER	6b. AR NUMBER	6c. TYPE OF REPORT	7. DOCUMENT DATE
DSTO-TR-0523	AR-010-203	Technical Report	April 1997

8. FILE NUMBER	9. TASK NUMBER	10. TASK SPONSOR	11. NO. OF PAGES	12. NO. OF REFERENCES
M1/9/167	Air 95/228	AIR OIC ASI-LSA	44	6

13. DOWNGRADING/DELIMITING INSTRUCTIONS

None

14. RELEASE AUTHORITY

Chief, Airframes and Engines Division

15. SECONDARY RELEASE STATEMENT OF THIS DOCUMENT

Approved for public release

OVERSEAS ENQUIRIES OUTSIDE STATED LIMITATIONS SHOULD BE REFERRED THROUGH DOCUMENT EXCHANGE CENTRE, DIS NETWORK OFFICE, DEPT OF DEFENCE, CAMPBELL PARK OFFICES, CANBERRA ACT 2600

16. DELIBERATE ANNOUNCEMENT

No Limitations

17. CASUAL ANNOUNCEMENT Yes

18. DEFTEST DESCRIPTORS

F-111 aircraft, holes, stress analysis, fatigue life

19. ABSTRACT

This investigation has been undertaken as part of a program of work having the aim of determining a suitable fatigue life enhancement option for the non-circular fuel flow vent hole # 13 in the wing pivot fitting of the F-111C aircraft. The stress analysis has been undertaken using two dimensional finite element methods assuming either elastic-perfectly plastic or strain hardening material behaviour models. The effect on critical plate stresses due to enhancement by cold expansion and interference fitting, used separately or together, has been quantified in the presence of representative cold proof test loading and a sample remote spectrum loading. For all enhancement cases considered, irrespective of material model, the stress response during the sample remote loading was linear, with a cyclic stress concentration factor of unity. Enhancement through combined cold expansion and interference fitting was considered a great deal better than interference fitting only. For example, the combined enhancement of 1.5% cold expansion followed by 0.5% interference fitting, as compared to 0.5% interference fitting only, led to a change in critical hoop stress from 350 MPa to -1080 MPa. These favourable results indicate that such an enhancement procedure would potentially be suitable for extending the fatigue life of the F-111 #13 fuel flow vent hole region, pending the results of an investigation on a non-circular hole geometry currently in progress.

TECHNICAL REPORT DSTO-TR-0523 AR-010-203 APRIL 1997

DSTO AUSTRALIA

AERONAUTICAL AND MARITIME RESEARCH LABORATORY
GPO BOX 4331 MELBOURNE VICTORIA 3001
AUSTRALIA, TELEPHONE (03) 9626 7000